ACS Infectious Diseases

pubs.acs.org/journal/aidcbc

Article

Newly Identified Antimicrobial Peptide Scymicrosin$_{7-26}$ from *Scylla paramamosain* Showing Potent Antimicrobial Activity Against Methicillin-Resistant *Staphylococcus aureus In Vitro* and *In Vivo*

Ying Zhou,[‖] Ying Wang,[‖] Xiangyu Meng, Ming Xiong, Xianxian Dong, Hui Peng, Fangyi Chen,* and Ke-Jian Wang*

Cite This: *ACS Infect. Dis.* 2025, 11, 1216−1232

Read Online

ACCESS | Metrics & More | Article Recommendations

ABSTRACT: Methicillin-resistant *Staphylococcus aureus* (MRSA) is a predominant pathogen causing skin and soft tissue infections, which significantly hinders the wound healing process and contributes to high mortality rates. The rise of multidrug-resistant bacteria, coupled with the limited availability of new antibiotics, underscores the pressing need for the development of innovative antimicrobial substances. Antimicrobial peptides (AMPs), with their multitargeted and rapid antimicrobial activity, are promising candidates to address this crisis. In this study, we identified a novel AMP, Scymicrosin$_{7-26}$, derived from *Scylla paramamosain*, which demonstrated potent antimicrobial activity against a variety of MDR strains, particularly MRSA. Confocal microscopy and transmission electron microscopy observations showed that Scymicrosin$_{7-26}$ bound to MRSA, and had a disruptive effect on cell walls and cell membranes, rapidly penetrating and killing MRSA. Notably, Scymicrosin$_{7-26}$ exhibited good stability under various ionic conditions, thermal stresses and certain serum concentration, had no obvious toxic effects on HaCaT cells, and its ability to penetrate HaCaT cells indicated its potential for intracellular targeted therapy. *In vitro*, Scymicrosin$_{7-26}$ significantly reduced the number of MRSA in HaCaT cells and inhibited intracellular MRSA proliferation. After verifying the low toxicity of Scymicrosin$_{7-26}$ *in vivo* in the Marine model organism—marine medaka (*Oryzias melastigma*), a wound model of MRSA-infected mice was made, and topical administration of Scymicrosin$_{7-26}$ in hypromellose gels could significantly reduce bacterial burden and promote wound closure. Histological analysis confirmed that Scymicrosin$_{7-26}$ alleviated tissue damage and was comparable to the effect of vancomycin treatment. Collectively, Scymicrosin$_{7-26}$ is promising for the treatment of MRSA wound infections and could be a valuable addition to the arsenal against antibiotic-resistant bacteria.

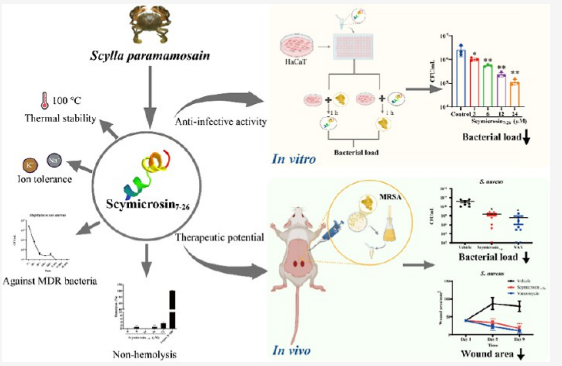

KEYWORDS: *Scylla paramamosain, antimicrobial peptides, Scymicrosin$_{7-26}$, MRSA, wound healing*

INTRODUCTION

The use of antibiotics has saved countless lives and created meaningful milestones in the medical revolution.[1,2] However, continuously misused or overused antibiotics resulted in the prevalence of MDR bacteria and subsequently caused tremendous death.[3] Annually, more than 700, 000 people died from MDR bacterial infection.[4] The ESKAPE group of pathogens—including *Enterococcus faecium*, *Staphylococcus aureus*, *Klebsiella pneumoniae*, *Acinetobacter baumannii*, *Pseudomonas aeruginosa*, and various *Enterobacter species*—encompasses key multidrug-resistant bacterial strains. Notably, *S. aureus* that is resistant to methicillin (MRSA) stands out as a major etiological agent in both hospital-acquired and community-onset infections.[5−7] In 2017, the World Health Organization (WHO) released a priority list to direct the research and development of novel antibiotics targeting antibiotic-resistant bacteria, with MRSA being categorized as a high-priority pathogen.[8] *S. aureus* frequently accounts for infections of the skin, capable of invading open wounds including those resulting from burns, ulcerations, and surgical incisions, potentially leading to life-threatening systemic infections.[9,10] However, the treatment of staphylococcal wound infections is facing challenge, as the ongoing dearth of effective drugs and MRSA strains exhibit resistance to

Received: January 16, 2025
Revised: April 11, 2025
Accepted: April 15, 2025
Published: April 23, 2025

https://doi.org/10.1021/acsinfecdis.5c00034
ACS Infect. Dis. 2025, 11, 1216−1232

topical antibiotics, such as fusidic acid and mupirocin,[11,12] posing an urgent need to exploit new antimicrobial agents.

Antimicrobial peptides (AMPs) are considered promising candidates for traditional antibiotics since AMPs have multitargeted, rapid and broad-spectrum antimicrobial activity with less prone to produce resistance.[13,14] The mud crab *Scylla paramamosain* has been recognized in recent years as a marine crustacean with abundant and unexploited antimicrobial resources.[15] Since 2006, multiple novel AMPs with demonstrated antimicrobial potential have been identified in *S. paramamosain*, such as Scyreprocin,[16] Sparamosin$_{26-54}$[17], and Spampcin$_{56-86}$.[18] However, the exploration of marine-derived AMPs targeting ESKAPE pathogens, especially MRSA, remains limited. Considering that most AMPs in clinical trials (e.g., omiganan, pexiganan, and DPK-060) are used for the treatment of chronic wound infections, and that MRSA is a common pathogen in wound infections,[11,19−22] it is worthwhile to further explore more marine-derived AMPs with potent anti-MRSA activity.

This study aims to investigate the antimicrobial potential of a newly identified peptide from *S. paramamosain* against ESKAPE pathogens, with particular focus on MRSA. Building on the established role of AMPs in wound infection treatment and considering the prominence of MRSA in such infections, we designed a comprehensive evaluation encompassing both *in vitro* antimicrobial characterization and an *in vivo* wound infection model. Our findings will contribute to the growing body of research on marine-derived AMPs and their potential application in the treatment of multidrug-resistant bacterial infectious diseases.

RESULTS

Characterization of Scymicrosin$_{7-26}$. We identified a new functional gene, named Scymicrosin (Genbank accession number: OP382459), from the transcriptional database of *S. paramamosain* previously constructed by our research group. Neither the nucleotide nor amino acid sequences of Scymicrosin has homologous with any other sequence in the existing online database. Scymicrosin encodes 56-amino acid residues, and contains α-helix and β-sheet structure (Figure 1A,B).

Based on the predictions of the CAMP$_{R3}$ database, we synthesized a truncated peptide Scymicrosin$_{7-26}$ from Scymicrosin. The peptide consists of 20 amino acids with 52.6% hydrophobic residues, which is indicative of its potential for membrane-disrupting properties (Figure 1A). The truncated peptide Scymicrosin$_{7-26}$ exhibits a typical α-helical structure (Figure 1C). The physicochemical properties of Scymicrosin$_{7-26}$ are summarized in Figure 1D, with a molecular weight of 2173.68 Da, a theoretical isoelectric point of 12.48, a net charge of +4, and a hydrophobic residue percentage of 52.6%. These characteristics suggest that Scymicrosin$_{7-26}$ is a cationic peptide with a strong propensity to interact with negatively charged bacterial membranes, which is a key mechanism of action for its antimicrobial activity.

Broad-Spectrum Antimicrobial Activity of Scymicrosin$_{7-26}$. As shown in Table 1, Scymicrosin$_{7-26}$ exhibits remarkable antibacterial activity against a variety of ESKAPE pathogens, with LL-37 serving as a positive control. The MIC and MBC values of Scymicrosin$_{7-26}$ were below 3 μM against *E. faecium* (CGMCC NO. 1.131), *S. aureus* (CGMCC NO. 1.2465), and *A. baumannii* (CGMCC NO. 1.6769). Additionally, Scymicrosin$_{7-26}$ demonstrated efficacy against clinically

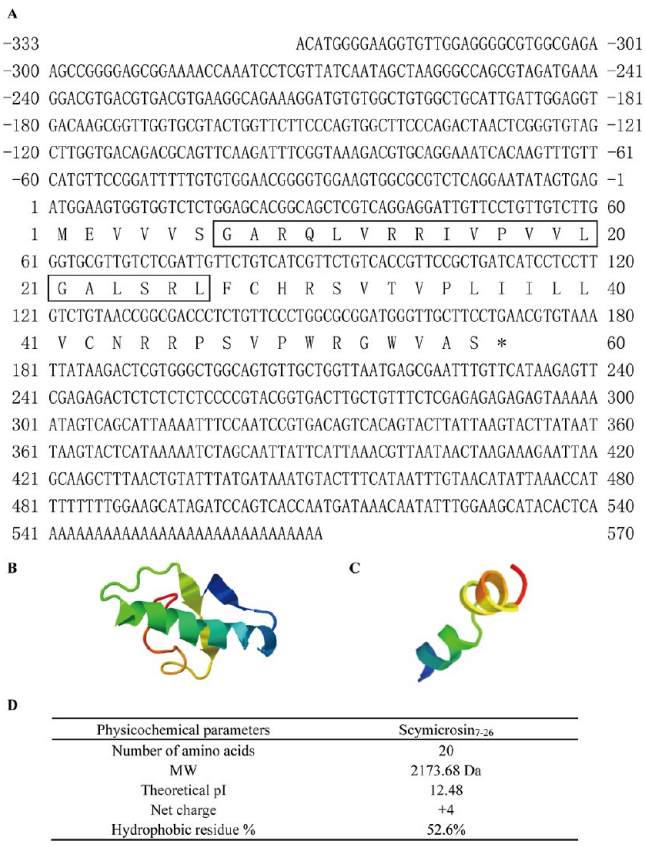

Figure 1. Characterization of Scymicrosin from *S. paramamosain*. (A) Full-length cDNA and deduced amino acid sequence of Scymicrosin. The nucleotide sequences are presented in the uppercase letters, and the corresponding amino acid sequences are shown below. (B) Tertiary structural model of Scymicrosin was predicted by the I-TASSER server. (C) Tertiary structural model of the truncated peptide Scymicrosin$_{7-26}$. (D) Physicochemical properties of Scymicrosin$_{7-26}$.

Table 1. Antimicrobial Activities of Scymicrosin$_{7-26}$[a]

microorganism	CGMCC NO	MIC (μM)	MBC (μM)	MIC (μM)
Gram-positive bacteria		Scymicrosin$_{7-26}$		LL-37
Staphylococcus aureus	1.2465	1.5−3	1.5−3	6−12
Enterococcus faecium	1.131	1.5−3	1.5−3	3−6
MRSA QZ19131		<1.5	<1.5	6−12
MDR *E. faecium* QZ18080		<3	<3	6−12
Gram-negative bacteria		Scymicrosin$_{7-26}$		LL-37
Acinetobacter baumannii	1.6769	<1.5	<1.5	3−6
Escherichia coli	1.2389	3−6	3−6	6−12
Pseudomonas aeruginosa	1.1785	6−12	6−12	6−12
MDR *A. baumannii* QZ18050		1.5−3	1.5−3	3−6
MDR *E. coli* QZ18109		<3	<3	6−12
MDR *P. aeruginosa* QZ19122		<3	<3	6−12
MDR *Klebsiella pneumoniae* QZ18106		3−6	3−6	6−12

[a]MIC: Minimum Inhibitory Concentration; MBC: Minimum Bactericidal Concentration. Antimicrobial results were uniformly expressed in the A-B format, where A is the highest concentration at which visible microbial growth was observed in the experiment and B is the lowest concentration at which no microbial growth was observed in the experiment.

https://doi.org/10.1021/acsinfecdis.5c00034
ACS Infect. Dis. 2025, 11, 1216−1232

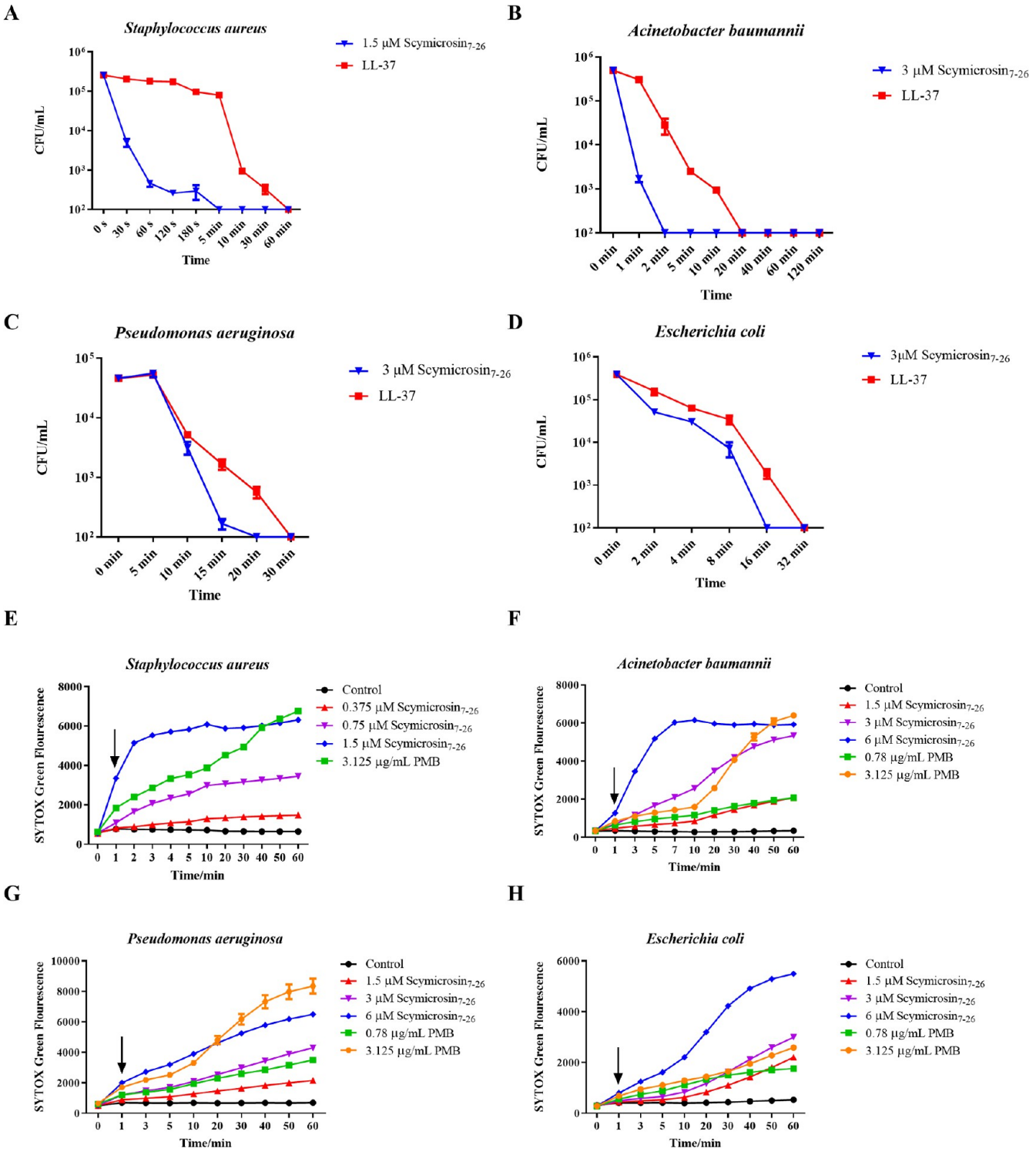

Figure 2. Effect of Scymicrosin$_{7-26}$ on the viability and membrane integrity of drug-resistant bacteria. (A–D) Time-killing curves of Scymicrosin$_{7-26}$ against clinical isolates of: (A) MRSA QZ19131, (B) *A. baumannii* QZ18050, (C) *P. aeruginosa* QZ19122, and (D) *E. coli* QZ18109. Bacterial cultures were grown to the mid logarithmic phase, washed, and resuspended in Mueller–Hinton broth. Aliquots were treated with Scymicrosin$_{7-26}$ at a concentration of 1 × MBC and incubated at 37 °C. At various time points, samples were diluted and plated on nutrient agar to determine the number of bacteria. (E–H) Effects of Scymicrosin$_{7-26}$ on bacterial membrane integrity, as measured by SYTOX Green fluorescence. (E) MRSA QZ19131, (F) *A. baumannii* QZ18050, (G) *P. aeruginosa* QZ19122, and (H) *E. coli* QZ18109 were suspended in HBSS containing SYTOX Green and treated with different concentrations of Scymicrosin$_{7-26}$. Fluorescence intensity was monitored using a multimode microplate reader.

isolated multidrug resistant (MDR) strains, including *E. faecium* QZ18080, MRSA QZ19131, *A. baumannii* QZ18050, *Escherichia coli* QZ18109, *P. aeruginosa* QZ19122, and *K. pneumoniae* QZ18106. The low MBC values of Scymicrosin$_{7-26}$ against these MDR strains highlight its potential as a therapeutic agent for infections caused by antibiotic-resistant

https://doi.org/10.1021/acsinfecdis.5c00034
ACS Infect. Dis. 2025, 11, 1216–1232

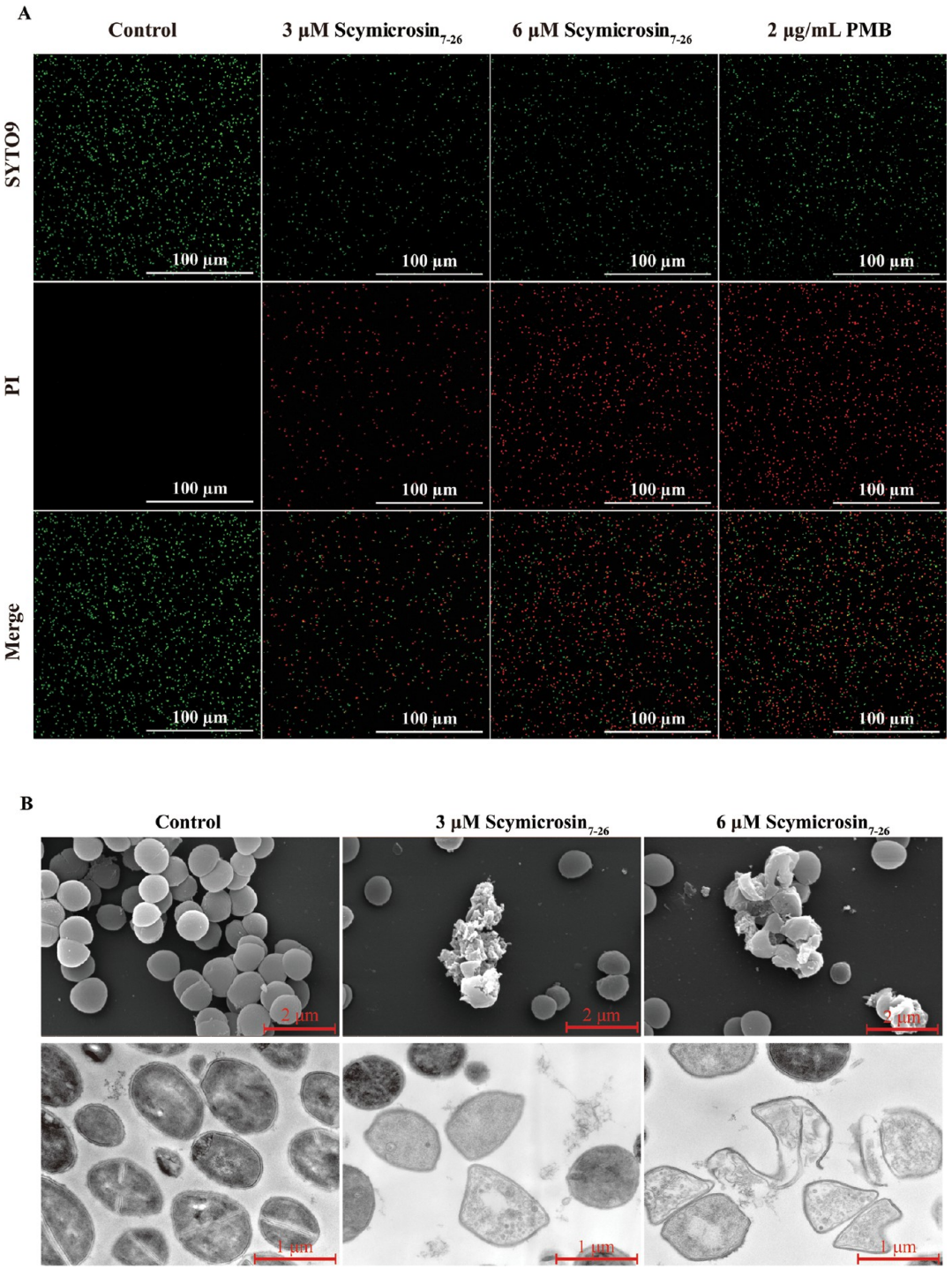

Figure 3. Scymicrosin$_{7-26}$ disrupts the membrane integrity of MRSA. (A) Confocal laser scanning microscopy (CLSM) images depicting the effect of Scymicrosin$_{7-26}$ on MRSA inner membrane permeability. Bacterial cells were stained with SYTO 9 and propidium iodide (PI). The presence of red fluorescence in the Scymicrosin$_{7-26}$-treated group indicates increased permeability, and PMB serves as a positive control for membrane disruption. (B) Morphological changes of MRSA after Scymicrosin$_{7-26}$ treatment, as observed by scanning electron microscopy (SEM) and transmission electron microscopy (TEM). MRSA exposed to Scymicrosin$_{7-26}$ for 30 min showed pronounced structural damage compared to the untreated control.

bacteria. These results are particularly important given the rising threat of MDR pathogens in clinical settings and the urgent need for novel antimicrobial agents to address these challenges.

Bactericidal Efficacy and Membrane Disruption of Scymicrosin$_{7-26}$ in Clinical MDR Bacterial Strains. The time-killing kinetic curve showed that Scymicrosin$_{7-26}$ had rapid bactericidal activity against clinical MDR strains, outperforming the LL37 in rapidity of action (Figure 2A–D). Notably, the viability of MRSA decreased rapidly upon exposure to Scymicrosin$_{7-26}$, with complete bacterial elimination achieved at a concentration of 1.5 μM within a short period of time, 5 min. The peptide also displayed remarkable

https://doi.org/10.1021/acsinfecdis.5c00034
ACS Infect. Dis. 2025, 11, 1216−1232

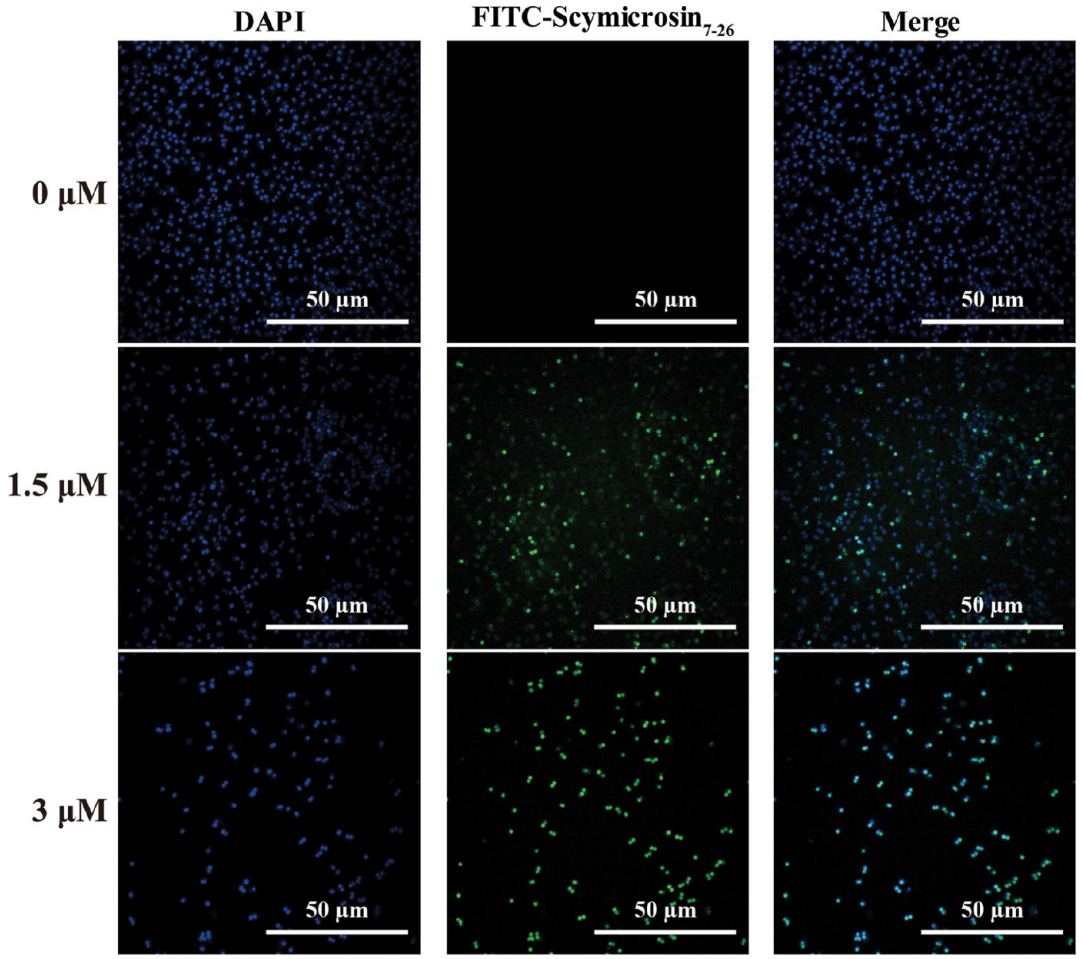

Figure 4. FITC-Scymicrosin$_{7-26}$ targets MRSA. MRSA QZ19131 cells were treated with FITC-Scymicrosin$_{7-26}$ at concentrations of 0, 1.5, and 3 μM for 1 h. After incubation, cells were stained with DAPI and observed under a confocal laser microscope.

efficacy against MDR *A. baumannii*, *E. coli* and *P. aeruginosa* within 2, 16 and 20 min, respectively (Figure 2A–D).

In an extension of these findings, we evaluated the effect of Scymicrosin$_{7-26}$ on bacterial membrane integrity. Scymicrosin$_{7-26}$ (1.5 μM) induced MRSA membrane permeabilization within 2 min, significantly faster than PMB-induced damage. In contrast, a higher concentration of 6 μM was required to elicit maximum fluorescence in MDR *A. baumannii*, *E. coli*, and *P. aeruginosa*, with corresponding times of 6, 60, and 60 min to peak fluorescence (Figure 2E–H). These results underscore that Scymicrosin$_{7-26}$ had a stronger membrane-disrupting potential against MRSA than the other MDR strains examined.

Scymicrosin$_{7-26}$ Induces Membrane Disruption and Cell Death in MRSA. We further evaluated the effect of Scymicrosin$_{7-26}$ on MRSA inner membrane permeability by staining with SYTO 9 and PI (Figure 3A). SYTO 9 labels all bacteria, whereas PI could only penetrate damaged bacterial membranes, bind to nucleic acids and emit red fluorescence. CLSM was used to analyze fluorescence colocalization. The control group exhibited intact bacterial membranes, whereas the positive control group treated with polymyxin B (PMB, 2 μg/mL) showed extensive PI labeling, indicating severe membrane damage. Treatment with 3 μM and 6 μM Scymicrosin$_{7-26}$ also resulted in extensive red fluorescent signals, indicating increased permeability and disruption of the MRSA inner membrane.

SEM and TEM images further showed that Scymicrosin$_{7-26}$ induced cell wall and membrane damage in MRSA, leading to cell death (Figure 3B). Scymicrosin$_{7-26}$-treated MRSA cells showed deformation, membrane disruption, and reduced electron density. At higher concentrations, Scymicrosin$_{7-26}$ also caused cell–wall disruption (Figure 3B). These findings together demonstrate the potent membrane disruption and bactericidal properties of Scymicrosin$_{7-26}$ against MRSA.

FITC-Scymicrosin$_{7-26}$ Targets MRSA. Scymicrosin$_{7-26}$ was proved to exhibit rapid membrane penetration and bactericidal activity against MRSA. Subsequently, the colocalization of the peptide with MRSA was analyzed using FITC-conjugated Scymicrosin$_{7-26}$. To rigorously assess the membrane penetration behavior of Scymicrosin$_{7-26}$, we employed FITC-Ahx (aminohexanoic acid) as a hydrophilic spacer between the fluorophore and peptide sequence, minimizing steric hindrance and nonspecific hydrophobic interactions. To spatially resolve its targeting mechanism, we performed confocal laser scanning microscopy on MRSA incubated with FITC-Scymicrosin$_{7-26}$. The peptide exhibited selective bacterial membrane localization, with fluorescence intensity concentration-dependent with concentration (Figure 4). At 3 μM, >90% of bacterial cells displayed circumferential FITC signal, consistent with membrane disruption observed via transmission electron microscopy (Figure 3B).

Stability, Cytotoxicity and Hemolytic Activity of Scymicrosin$_{7-26}$. The stability assessment of Scymicrosin$_{7-26}$

https://doi.org/10.1021/acsinfecdis.5c00034
ACS Infect. Dis. 2025, 11, 1216–1232

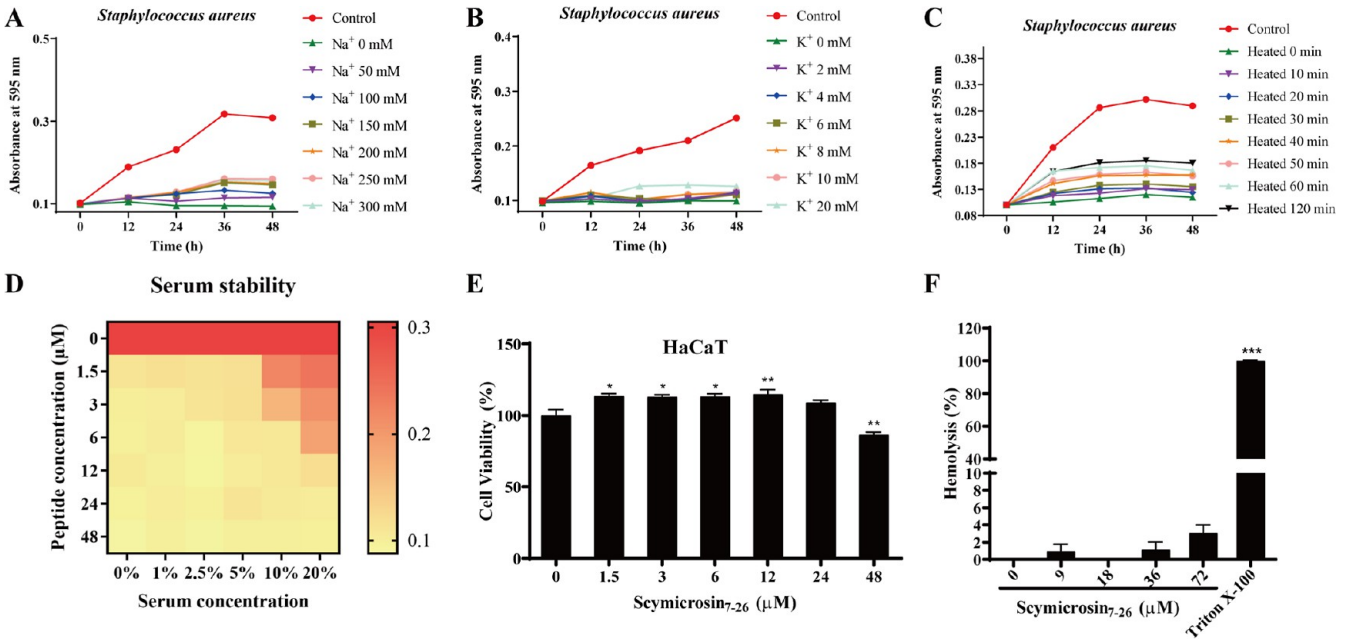

Figure 5. Stability, cytotoxicity and hemolytic activity of Scymicrosin$_{7-26}$ were evaluated. (A) Evaluation of the antibacterial activity of Scymicrosin$_{7-26}$ against MRSA at varying sodium ion concentrations. (B) Determination of the antibacterial efficacy of Scymicrosin$_{7-26}$ against MRSA under different potassium ion concentrations. (C) The effect of 100 °C heat treatment on the antimicrobial activity of Scymicrosin$_{7-26}$ against MRSA was analyzed. (D) Antibacterial effect of Scymicrosin$_{7-26}$ on MRSA at different serum concentrations. (E) Measurement of the cytotoxic effect of Scymicrosin$_{7-26}$ on HaCaT cells in serum-free DMEM. (F) Evaluation of the hemolytic potential of Scymicrosin$_{7-26}$ on mouse erythrocytes, with 0.9% saline as a negative control and 0.1% Triton X-100/saline as a positive control. *$p < 0.05$, **$p < 0.01$, ***$p < 0.001$.

included evaluating its antimicrobial activity under various treatment conditions. Scymicrosin$_{7-26}$ remained highly active at Na^+ concentrations below 300 mM (Figure 5A). Similarly, potassium (K^+) concentrations below 20 mM had little effect on the peptide's activity (Figure 5B). The thermal stability of Scymicrosin$_{7-26}$ was shown in Figure 5C, demonstrating that exposure to temperatures of 100 °C for durations ranging from 0 to 120 min did not significantly impact its activity. The stability of Scymicrosin$_{7-26}$ in different serum concentrations was systematically evaluated by MIC assay. The stability of Scymicrosin$_{7-26}$ at different serum concentrations was evaluated by the MIC assay. The results showed that the MIC value of Scymicrosin$_{7-26}$ against MRSA remained unchanged at serum concentration ≤5%, whereas the MIC value increased 4-fold and 8-fold at serum concentrations of 10% and 20%, respectively (Figure 5D). This suggested that Scymicrosin$_{7-26}$ might be effective in biological settings where local serum protein levels are reduced, such as topical application or infected tissues.

Beyond assessing the stability of AMPs, evaluating their biocompatibility is crucial for advancing their practical applications. Scymicrosin$_{7-26}$ showed no cytotoxicity and no hemolytic activity against HaCaT cells at concentrations below 48 μM (Figure 5E,F).

Cell Membrane Penetration Activity of Scymicrosin$_{7-26}$. In addition to their disruptive effects on bacterial membranes, certain cationic peptides are capable of penetrating cell membranes, which endows them with potential applications in intracellular targeted therapy. We have demonstrated that Scymicrosin$_{7-26}$ can target bacteria by traversing bacterial membranes. Subsequently, we further investigate the membrane penetration activity of Scymicrosin$_{7-26}$ using HaCaT cells. As shown in Figure 6A, 1.5 μM Scymicrosin$_{7-26}$ was able to colocalize with HaCaT cells, and the fluorescence signal of the peptide in the cytoplasm increased with the increase of the peptide concentration, indicating that the uptake of Scymicrosin$_{7-26}$ by the cells was concentration-dependent. Notably, fluorescent signals were also detected in the nuclei of cells treated with higher concentrations of Scymicrosin$_{7-26}$. These results suggested that Scymicrosin$_{7-26}$ could penetrate the cell membrane at low concentrations with good cellular penetration. Collectively, these findings led us to speculate that Scymicrosin$_{7-26}$ has the potential for intracellular targeted bactericidal action.

Antibacterial Effect of Scymicrosin$_{7-26}$ against MRSA Extracellular and Intracellular Infections. Keratinocytes are the most abundant cell type in the epidermis. We preliminarily demonstrated that the viability of HaCaT cells was not affected when Scymicrosin$_{7-26}$ concentrations was below 24 μM (Figure 4D). There is compelling evidence that *S. aureus* can enter host cells and evade immune attacks.[23] To further explore whether Scymicrosin$_{7-26}$ possesses the ability to target and kill intracellular bacteria, we assessed its anti-infective ability in HaCaT cells using two experimental designs: MRSA pretreatment and Scymicrosin$_{7-26}$ pretreatment. After 1 h of pretreatment, the cells were coincubated with different concentrations of Scymicrosin$_{7-26}$ (3, 6, 12, and 24 μM) or MRSA for 12 h (Figure 6B,C). The results showed that, in the case of MRSA pretreatment, Scymicrosin$_{7-26}$ significantly reduced the number of extracellular and intracellular MRSA in HaCaT cells compared to the control group, and this effect was markedly concentration-dependent (Figure 6B). In the case of Scymicrosin$_{7-26}$ pretreatment, 24 μM Scymicrosin$_{7-26}$ significantly reduced the number of extracellular MRSA bacteria. Interestingly, compared to the control group, Scymicrosin$_{7-26}$ at concentrations ranging from 3 to 24 μM significantly reduced the number of intracellular MRSA bacteria (Figure 6C). Collectively, these findings indicated that

https://doi.org/10.1021/acsinfecdis.5c00034
ACS Infect. Dis. 2025, 11, 1216−1232

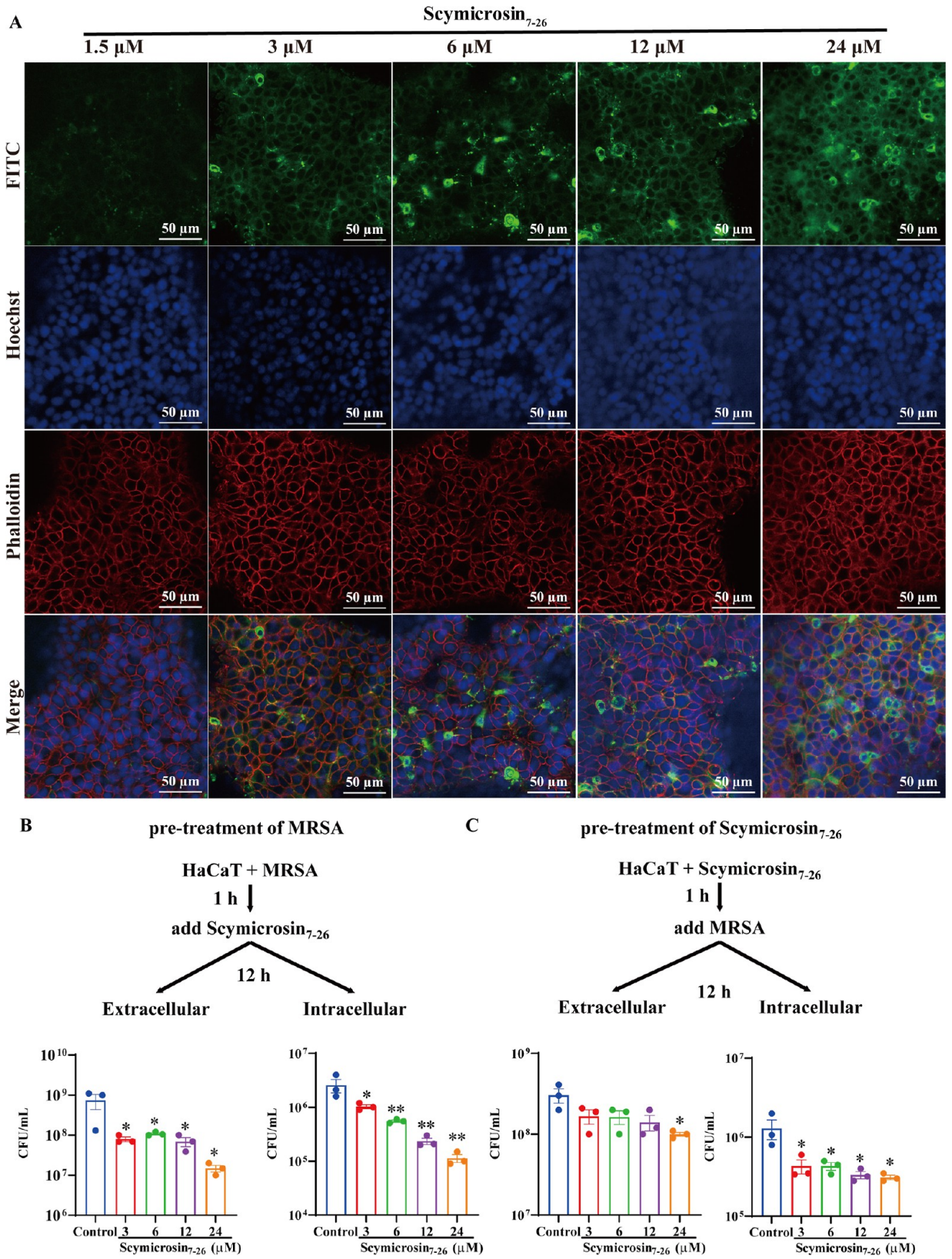

Figure 6. Cell membrane penetration activity and antibacterial effect of Scymicrosin$_{7-26}$ against MRSA extracellular and intracellular infections. (A) HaCaT cells were treated with Scymicrosin$_{7-26}$ at concentrations ranging from 1.5 to 24 μM. Cellular uptake was observed using FITC-labeled Scymicrosin$_{7-26}$ (green), Hoechst 33,342 (blue) for nuclear staining, and rhodamine-labeled phalloidin (red) for highlighting the cytoskeleton. The merged images show that the higher the concentration, the higher the internalization of Scymicrosin$_{7-26}$. (B) HaCaT cells pretreated with MRSA for 1 h were exposed to Scymicrosin$_{7-26}$ at concentrations of 3, 6, 12, and 24 μM. Extracellular and intracellular bacterial loads were assessed after 12 h. (C) HaCaT cells pretreated with Scymicrosin$_{7-26}$ at concentrations of 3, 6, 12, and 24 μM for 1 h were exposed to MRSA after 12 h. Extracellular and intracellular bacterial loads were assessed after 12 h. *$p < 0.05$, **$p < 0.01$, ***$p < 0.001$.

https://doi.org/10.1021/acsinfecdis.5c00034
ACS Infect. Dis. 2025, 11, 1216−1232

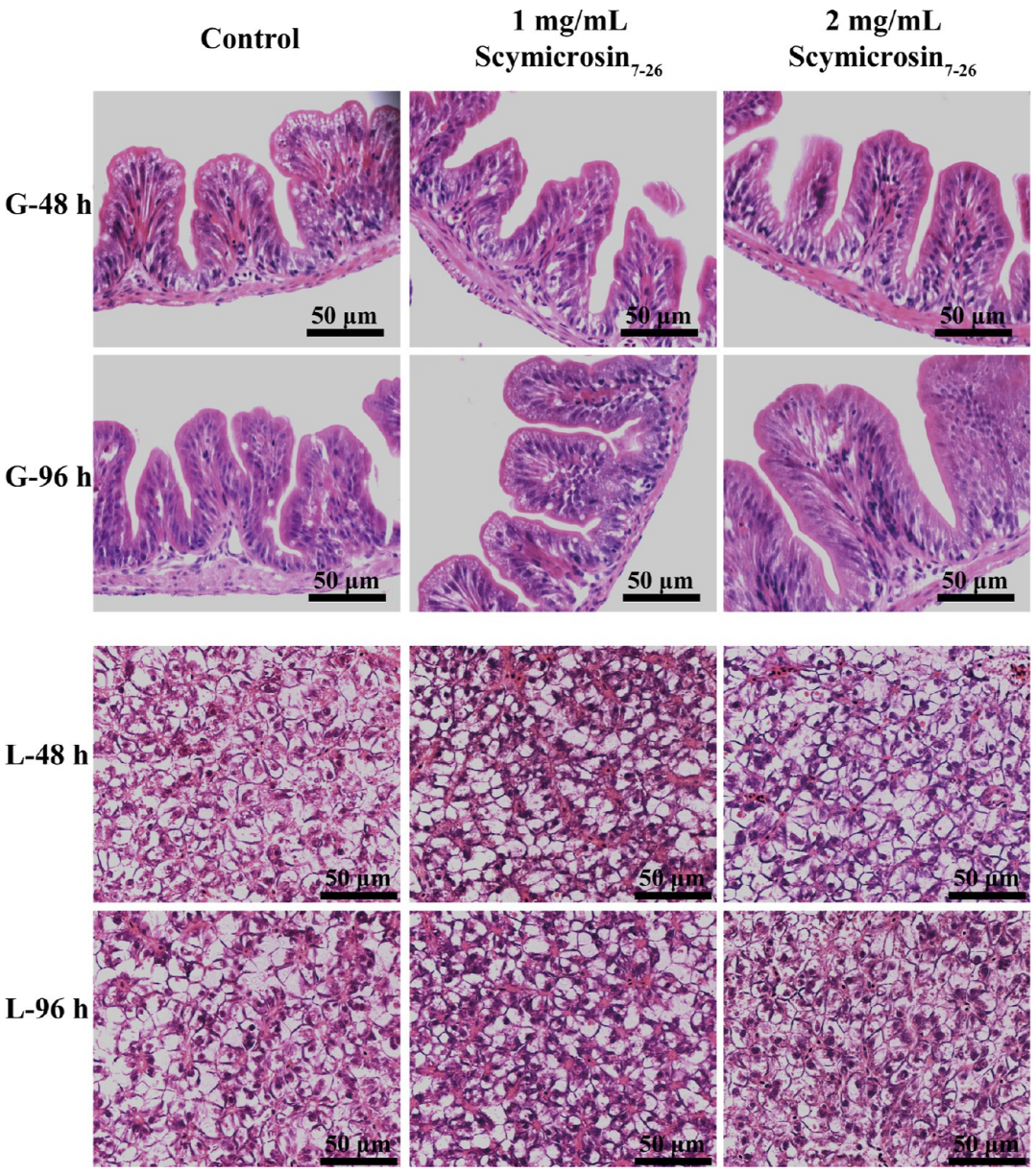

Figure 7. Effects of different concentrations of Scymicrosin$_{7-26}$ on liver and intestinal histology of marine medaka. The effects of Scymicrosin$_{7-26}$ at concentrations of 1 and 2 mg/mL on the histology of marine medaka intestine and liver were assessed at 48 and 96 h. The control group served as a reference for comparison. Intestinal tissue sections (G-48 and G-96 h) were used to evaluate villus structure and epithelial cell arrangement, and liver tissue sections (L-48 and L-96 h) were analyzed to assess liver cell morphology and tissue organization.

Scymicrosin$_{7-26}$ could not only prevent MRSA from invading cells, but also enter the cells to exert bactericidal activity. Furthermore, treatment with Scymicrosin$_{7-26}$ appeared to be more effective after MRSA infection.

***In Vivo* Toxicity of Scymicrosin$_{7-26}$.** Scymicrosin$_{7-26}$ is a peptide derived from *S. paramamosain*. Prior to conducting experiments in the murine model, we performed a *in vivo* toxicity assessment using the marine medaka (*Oryzias melastigma*). This species has been well-established as a reliable model for toxicity evaluation of marine compound.[24] In the results, 2 mg/mL of Scymicrosin$_{7-26}$ did not show any significant adverse effects or cause mortality in medaka during a two-week observation period. Histopathological examinations of the liver and intestine did not reveal any obvious lesions or abnormalities (Figure 7).

Efficacy of Scymicrosin$_{7-26}$ on Wound Infection. We successfully constructed a murine model of skin wound infection caused by MRSA. The results showed that both treatments of Scymicrosin$_{7-26}$ and vancomycin significantly reduced the bacterial loads and prompted wound closure (Figure 8). After treatment with Scymicrosin$_{7-26}$ and vancomycin, the number of MRSA isolated from the wound tissue decreased from 1.5×10^{11} (mean) to 2.2×10^{8} (mean) and 4.1×10^{7} CFU/mL (mean), respectively (Figure 8A). On day 1, the average wound areas of each group were 39.27 mm^2. After 4 days of infection, the wound area in the vehicle group expanded to 86.99 mm^2, while it decreased to 33.89 mm^2 (The wound shrinkage rate, WCR: 13.7%) and 22.88 mm^2 (WCR: 41.73%) in the Scymicrosin$_{7-26}$ and vancomycin-treated groups, respectively. On day 9, the wound area in the vehicle group was 79.62 mm^2, while it continued to decrease to 17.83

https://doi.org/10.1021/acsinfecdis.5c00034
ACS Infect. Dis. 2025, 11, 1216−1232

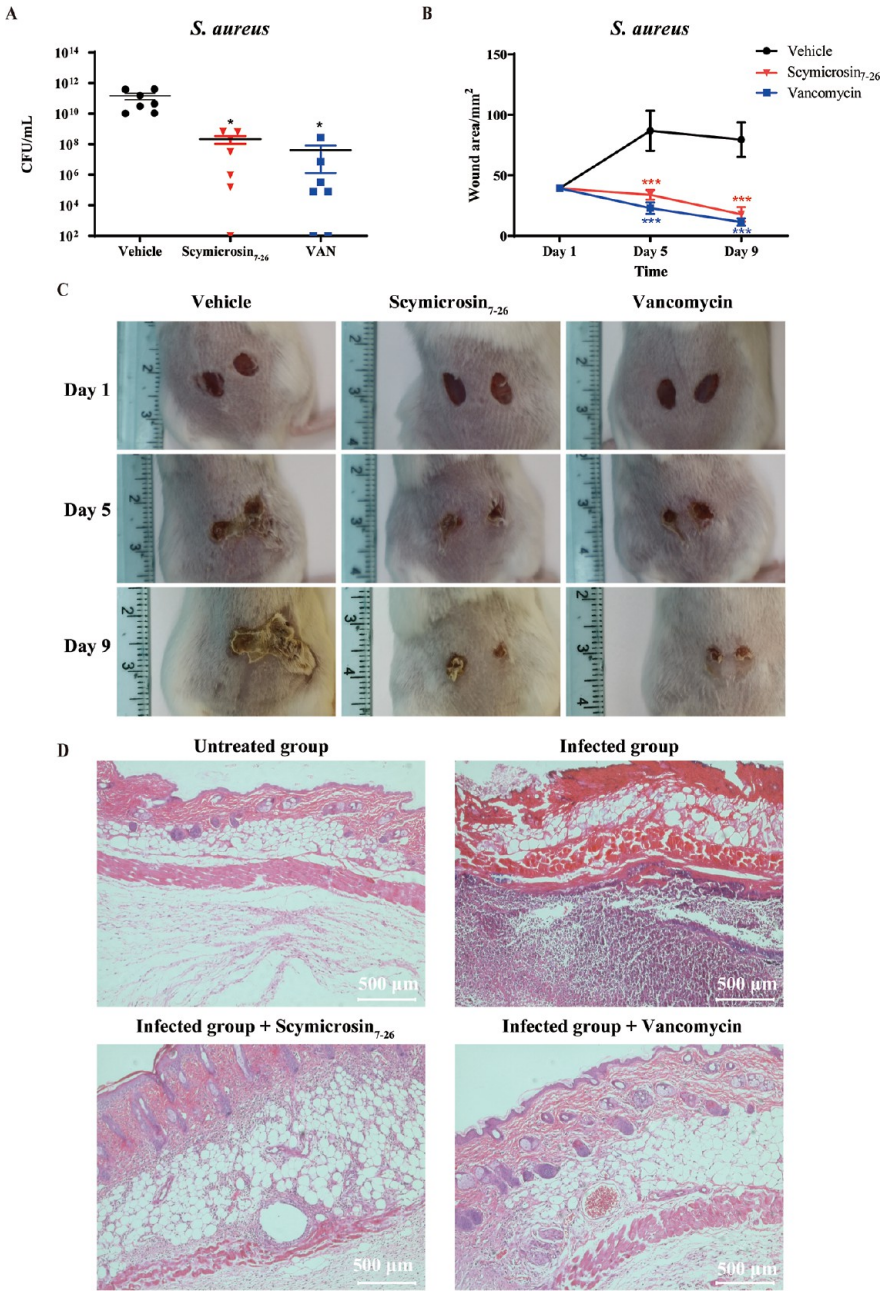

Figure 8. Efficacy of Scymicrosin$_{7-26}$ in treating MRSA-induced wound infection in Mice (n = 7) (A) Bacterial load in infected wounds. The statistical differences were analyzed by analysis of variance (ANOVA) and Dunnett's posttest. (B) Wound area of different treatments. The wound areas were calculated by ImageJ software and statistical differences were analyzed by two-way ANOVA. *p < 0.05, **p < 0.01, ***p < 0.001. (C) Representative image of wounds. Full-thickness excisional wounds (5 mm diameter) were made on the dorsal surfaces of mice, and 25 μL of MRSA (10^9 CFU/mL) was added to each wound. Twenty-five μL of 2% Hypromellose ointment containing sterile water (the control group) or 0.2% (w/w) Scymicrosin$_{7-26}$ or 0.1% (w/w) vancomycin was added to each wound 30 min after infection, followed by additional treatments on days 2 to 4 (12 h intervals). (D) Histological analysis of murine skin by HE staining.

mm^2 (WCR: 54.59%) and 11.49 mm^2 (WCR: 70.74%) in the treatment of Scymicrosin$_{7-26}$ and vancomycin, respectively (Figure 8B). Histological analysis showed that MRSA infection caused severe tissue damage and massive infiltration of inflammatory cells compared to the healthy tissues, while treatment with Scymicrosin$_{7-26}$ and vancomycin alleviated the tissue damage (Figure 8C,D). These results suggested a promising application of Scymicrosin$_{7-26}$ in the prevention of staphylococcal wound infections.

DISCUSSION

The prevalence of MDR bacteria has diminished the efficacy of traditional antibiotics, underscoring the urgency to explore novel antimicrobial agents, such as AMPs, to combat the escalating drug resistance crisis.[25,26] In this study, a novel cationic AMP Scymicrosin$_{7-26}$ was identified, which is composed of 20 amino acid residues, rich in hydrophobic residues, and exhibits a typical α-helical structure. The most common microbicidal mechanism of AMPs is via targeting membranes and causing membrane permeabilization.[11,27] The

https://doi.org/10.1021/acsinfecdis.5c00034
ACS Infect. Dis. 2025, 11, 1216−1232

rapid bactericidal efficacy of AMPs may shorten the duration of antimicrobial therapy and reduce the incidence of antibiotic-resistant gene mutations.[1,10] Notably, Scymicrosin$_{7-26}$ demonstrated superior rapid bactericidal kinetics compared to LL-37 (12-fold faster against MRSA at the same MIC multiplier), establishing its advantage in acute infection scenarios where immediate bactericidal action is critical (Figure 2A−D). TEM observations showed that Scymicrosin$_{7-26}$ disrupted cell walls and membranes, leading to the leakage of cell contents and eventually the death of MRSA. We further confirmed that FITC-Scymicrosin$_{7-26}$ could bind to MRSA and accumulate in MRSA. Upon targeted binding of AMPs to the outer membrane of pathogens, a subset of these peptides penetrates the outer membrane, and the extent of inner membrane permeation increases as more AMP molecules arrive.[28] Both the binding activity of AMPs to bacteria and its continued accumulation in bacteria enhance the membrane−disruption activity.

The varied amino acid sequences and structures of AMPs render them less prone to bacterial resistance. Nonetheless, there is variability among AMPs regarding their efficacy, stability, and toxicity.[27,29,30] Considering the prevalence of sodium and potassium ions in biological systems, especially in high-salt environments such as certain body fluids and marine environments, the tolerance of AMPs to sodium and potassium ions is an essential feature of their potential as antimicrobial agents.[31−35] The ionic tolerance of AMPs directly affects their effectiveness and stability in practical applications. The interaction between these ions and AMPs affects the interaction of AMPs with bacterial cell membranes, which in turn affects their antimicrobial activity.[31] In clinical applications, AMPs must act in body fluids (such as blood, urine, or wound exudates) containing different concentrations of sodium and potassium ions, so the ion tolerance of AMPs is critical for their therapeutic efficacy.[33] At the same time, serum has a complex composition, containing a large number of plasma proteins and proteases, which will affect the antibacterial activity of AMPs.[36] The cytotoxicity and hemolytic activity of AMPs need to be determined to evaluate their safety and feasibility as therapeutic agents.[33,35,37] In the present study, we assessed the stability and safety profiles of Scymicrosin$_{7-26}$. Our findings indicated that Scymicrosin$_{7-26}$ remained highly active at sodium concentrations up to 300 mM or potassium concentrations up to 20 mM. The MIC of Scymicrosin$_{7-26}$ remained stable at 5% serum but increased 4- to 8-fold increase at 10% and 20% serum concentrations. The results indicated that it was partially tolerant to serum, which may be attributed to a combination of its physicochemical properties. Such as the net positive charge (+4) and balanced hydrophobicity (52.6%), studies suggested that they may reduce nonspecific protein interactions.[38,39] Furthermore, its unique α-helical topology may enhance its resistance to proteolytic degradation in complex biological matrices.[40] Moreover, exposure to elevated temperatures did not compromise Scymicrosin$_{7-26}$ activity. In the safety evaluation, Scymicrosin$_{7-26}$ showed no cytotoxicity and no hemolytic activity at concentrations up to 48 μM. Collectively, these findings suggest that Scymicrosin$_{7-26}$ possesses favorable stability and biocompatibility.

It has been reported that *S. aureus* has a dramatic effect on the proliferation and migration of keratinocyte and slows down the wound healing process.[6] The interaction of *S. aureus* with keratinocytes is critical for its colonization and infection processes, since keratinocytes are the most abundant cell type in the epidermis.[23] *S. aureus* is able to enter host cells and evade immune attacks, making conventional antibiotics less effective.[41] Several studies have shown that AMPs can penetrate mammalian cells without membrane permeabilization, e.g., temporins A and B kill intracellular *S. aureus* in HaCaT cells at a nontoxic concentrations.[23] Our research findings unveiled a dual mechanism of action of Scymicrosin$_{7-26}$: it not only effectively disrupted bacterial membranes, but also able penetrated HaCaT cell membrane at nontoxic concentrations, demonstrating the potential for its intracellular targeting and bactericidal activity. This finding highlights the multifaceted advantages of Scymicrosin$_{7-26}$ as a novel antimicrobial agent, and provides robust support for its application in combating antibiotic-resistant infections.

Increasing incidence of MDR bacterial infection in wounds is a major concern, exacerbated by the resistance of MRSA strains to topical antibiotics.[11] Some AMPs were efficacy against wound infections, such as DRGN-1[42] or SHAP1[43] which significantly reduced the size and bacterial counts of wounds in *S. aureus*-infected mice. However, many AMPs, such as LL-37 and β-defensins, often encounter diminished functionality at physiological salt concentrations and are subject to modulation by host factors, which can impact their overall effectiveness.[20] Therefore, it is necessary to enhance the biological activity of AMPs. In recent times, the incorporation of antimicrobial substances into wound dressings has become a practical approach for managing infections in wounds.[44] Hypromellose gels are commonly used for *in vivo* drug delivery and rehydration in dry eyes, which are considered relatively safe for topical application.[45] AMP in hypromellose gels has been shown to have bactericidal effects, such as P60.4Ac[45] and SAAP-148[46]. P60.4Ac was found to be effective in eradicating MRSA from cultured skin and airway epithelial surfaces when formulated in a gel, and its peptide content was analyzed by HPLC in hypromellose gel containing 0.5% (w/w) P60.4Ac. The peptide can be stably stored in the gel for up to 3 months without affecting its bactericidal activity.[45] Similarly, SAAP-148, another antimicrobial peptide, was shown to combat drug-resistant bacteria and biofilms when incorporated into a hypromellose gel.[46] These studies support the feasibility of using hypromellose gels as a delivery system for antimicrobial peptides. In our study, the therapeutic efficacy of Scymicrosin$_{7-26}$ in the hypromellose gel was evident with a significant improvement in wound healing and a remarkable reduction in bacterial loads. This suggests that the peptide was effectively delivered to the site of infection and exerted its antimicrobial activity. Importantly, post-treatment tissue analysis showed no residual gel matrix at the wound sites, confirming complete degradation of the formulation and in situ release of the peptide. This observation is consistent with the hypromellose's known reverse thermal gelation behavior, where gel dissolution occurs through gradual hydration at physiological temperatures.[47] In future studies, we will incorporate peptide release analysis to further characterize the performance of the hypromellose gel as a delivery vehicle for Scymicrosin$_{7-26}$. This will help us refine the formulation and enhance the therapeutic potential of the antimicrobial peptide. In addition, other carriers—nanoparticles or microparticles (such as polymeric carriers and inorganic materials) can help facilitate the absorption of AMPs, enhance antibacterial activity, and reduce toxicity.[48] For example, LL-37 was encapsulated in liposomes or aurein-

https://doi.org/10.1021/acsinfecdis.5c00034
ACS Infect. Dis. 2025, 11, 1216−1232

Table 2. Primer Sequences

primers	sequence (5′−3′)
Scymicrosin-5′-R1	ACAACGCACCCAAGACAACAGGA
Scymicrosin-5′-R2	CGCCAGGGAACAGAGGGTCGCCG
Scymicrosin-3′-F1	CATTGATTGGAGGTGACAAGCGGT
Scymicrosin-3′-F2	GGATTTTTGTGTGGAACGGGGTGG
long primer	CTAATACGACTCACTATAGGGCAAGCAGTGGTATCAACGCAGAGT
NUP	AAGCAGTGGTATCAACGCAGAGT

derived peptides were formulated in pegylated phospholipid micelles.[49,50] Similar to the results of the present study, the combination of antimicrobial peptide CM11 and fibrin glue (FG) can significantly promote wound repair in a rat wound model. After 14 days, the wound shrinkage rate in the FG-P treated group reached 80%, which was significantly higher than that of the control group (40%).[51] In addition, some AMPs exhibit synergistic interactions when combined with other AMPs, surfactants, and conventional antibiotics, and the synergistic effects can improve antibacterial activity.[10,52] In this study, Scymicrosin$_{7-26}$ had a potential protective effect on wounds and prevention of MRSA-infection, which could be further enhanced by optimizing the delivery system or combining it with other antimicrobial agents to increase the efficacy of Scymicrosin$_{7-26}$ and expand its application. Finally, the antimicrobial activity revealed in this study is based exclusively on *in vitro* experimental systems and a mouse wound healing model, which is different from the physiological environment of systemic infection therapy. Although *in vitro* assays allow precise control of variables, they cannot replicate the complex immune−metabolic interactions *in vivo*. Therefore, the current data support the potential of Scymicrosin$_{7-26}$ as a topical anti-infective agent, but its feasibility for systemic administration requires further validation through pharmacokinetic studies. Additionally, the limited stability of Scymicrosin$_{7-26}$ in serum underscores its suitability for the development of topical therapeutic agents, but also highlights the challenges of systemic drug delivery. Future efforts should focus on advanced delivery strategies, such as nanoparticle encapsulation to improve its stability in high serum environments, circumvent protease degradation, and maintain bioactive concentrations, thereby expanding its therapeutic applicability.

CONCLUSIONS

Scymicrosin$_{7-26}$ exhibited potent and broad-spectrum antimicrobial activity against MDR strains, especially effective against MRSA. Our findings showed that Scymicrosin$_{7-26}$ not only rapidly kill MRSA, but also excerted anti-infective effects in HaCaT cells and significantly promoted wound healing while reducing the bacterial loads in wounds of MRSA-infected mice. The stability of Scymicrosin$_{7-26}$ under physiologically relevant conditions and its ability to penetrate HaCaT cells highlighted its potential for both extracellular and intracellular therapeutic applications. These results contribute to the development of new antimicrobial strategies to combat the resistance crisis posed by MRSA and lay the groundwork for future applications of AMPs in biomedical and related fields. The multifaceted attributes of Scymicrosin$_{7-26}$, including its stability, cellular penetration, and antimicrobial potency, position it as a promising candidate for further development in the fight against antibiotic-resistant infections.

MATERIALS AND METHODS

Animal or Tissues Preparation. Mud crabs of the species *S. paramamosain*, weighing approximately 300 ± 10 g, were sourced from Zhangpu Fish Farm in Fujian, China. Subsequently, their tissues and organs were harvested for the purpose of RNA extraction.

The marine medaka (*O. melastigma*) have been stably bred for more than 10 generations at the Marine Medaka Breeding Center of the College of Ocean and Earth Sciences, Xiamen University. Breeding conditions: the salinity of the artificial seawater was 30‰, the breeding temperature was 28 ± 1 °C, the lighting was controlled to start at 8:00 AM and end at 10:00 PM every day, simulating the photoperiod (day/night = 14:10), and the medaka were fed twice a day with brine shrimp, at 9:00 AM and 17:00 PM. Before the experiment, they were kept in temporary cultivation for more than 48 h and feeding was stopped.

Female BALB/c mice, aged between six and 8 weeks and free of specific pathogens (SPF), were procured from Beijing Vital River Laboratory Animal Technology Co., Ltd., located in Beijing, China. These mice were housed in individual ventilated cages (IVCs) under a controlled environment with a 12 h light/dark cycle at ambient temperature. The experimental procedures involving these mice were granted approval by the Laboratory Animal Management and Ethics Committee at Xiamen University, with the reference number XMULAC20230090, and adhered to the guidelines set forth in the National Research Council's publication, "Guide for the Care and Use of Laboratory Animals".

Amplification and Bioinformatics Analysis of Scymicrosin. The transcriptome database of *S. paramamosain* infected with Vibrio alginolyticus, previously established by our research group, was used to screen for differentially expressed genes with unknown functions. A significantly upregulated gene was identified, and its full-length cDNA was obtained using RACE-PCR with primers listed in Table 2. The related reagents were same as previously reported.[53] The obtained fragments were cloned into pMD18-T Vector (Takara, China) and sequenced by Bioray biotechnology (China). Sequence alignment showed no homology to any known sequences in existing databases, which confirmed its novelty, naming it Scymicrosin. Antimicrobial potential of the encoded peptide was analyzed using the antimicrobial peptide database CAMPR$_3$. The physicochemical properties of the encoded peptide, including net charge and hydrophobicity, were calculated using the ProtParam tool on the Expasy server. PSIPRED and I-TASSER was used to predict the secondary structure. Detailed parameters and versions of the databases and software used were summarized in Table 3.

Synthesis of Peptide. The truncated peptide Scymicrosin$_{7-26}$ (sequence: GARQLVRRIVPVVLGALSRL-NH2) was designed based on its net charge (+4) and hydrophobicity (52.6%), which are typical properties of AMPs, as well as the

https://doi.org/10.1021/acsinfecdis.5c00034
ACS Infect. Dis. 2025, 11, 1216−1232

Table 3. Website and Application of Related Database or Analysis Software

database or analysis software	application	web site
NCBI BLAST	analyzation of homology and similarity	https://blast.ncbi.nlm.nih.gov/Blast.cgi
ORF finder	prediction of open reading frame	https://www.ncbi.nlm.nih.gov/orffinder/
Expasy	computation of pI/Mw	https://web.expasy.org/compute_pi/
PSIPRED 4.0	prediction of secondary structure	http://bioinf.cs.ucl.ac.uk/psipred/
I-TASSER	prediction of tertiary structure	https://zhanglab.ccmb.med.umich.edu/I-TASSER/
$CAMP_{R3}$	prediction of antimicrobial region	http://www.camp3.bicnirrh.res.in/index.php

antimicrobial domain predicted in the $CAMP_{R3}$ database (threshold scores >0.8). $Scymicrosin_{7-26}$ and FITC-$Scymicrosin_{7-26}$ (*N*-terminus was labeled with fluorescein isothiocyanate (FITC)) were chemically synthesized by Genscript (Nanjing, China). The peptides were dissolved in sterile ultrapure water and subsequently preserved at a temperature of −20 °C.

Strains and Cultivation. The MDR strains clinical isolates, including *E. faecium* QZ18080, *A. baumannii* QZ18050, MRSA QZ19131, *P. aeruginosa* QZ19122, *E. coli* QZ18109 and *K. pneumoniae* QZ18106, were isolated from clinical specimens at the Second Affiliated Hospital of Fujian Medical University (Fujian, China), while other strains were procured from China General Microbiological Culture Collection Center (CGMCC). Cultivation of these bacterial strains was conducted in nutrient broth (NB) at a temperature of 37 °C. All associated experiments were conducted in strict accordance with the biosecurity protocols and institutional safety measures as stipulated by Xiamen University.

Antimicrobial Assay. Determination of the minimum inhibitory concentration (MIC) and the minimum bactericidal concentration (MBC) was accomplished using the broth dilution technique. The MIC represents the lowest concentration of the peptide that fully suppresses bacterial proliferation, whereas the MBC denotes the concentration necessary to eradicate 99.9% of the microbial population.[17] Briefly, exponential phase of bacteria was harvested and adjusted to approximately 10^6 CFU/mL with Mueller−Hinton (MH) broth. Different concentrations of $Scymicrosin_{7-26}$ were added and then cultured at 37 °C for 24 h. The antimicrobial peptide cathelicidin LL-37 was selected as a positive control (Jill Biochemistry, China). Each experiment was conducted independently three times.

Time-Killing Curves. The time-killing kinetics of the peptides against bacterial strains were conducted following the same protocol as the antimicrobial susceptibility testing. Each of the four MDR strains was incubated with $Scymicrosin_{7-26}$ at its corresponding 1 × MIC. Following incubation at specified intervals, the bacterial suspensions were appropriately diluted and then spread on nutrient broth (NB) agar plates for overnight incubation, and counted for colony forming units (CFU). The antimicrobial peptide cathelicidin LL-37 was selected as a positive control (Jill Biochemistry, China) at a final concentration of 1 × MIC.[54] Each experiment was conducted independently three times.

Membrane Permeabilization Assay. The membrane permeabilization was measured with SYTOX Green stain (Invitrogen, United States) as previously reported with some modifications.[11] 10^8 CFU/mL of microorganisms were suspended in HBSS containing 10 μM SYTOX Green (except for *S. aureus*, which required only 1 μM SYTOX Green), and incubated with $Scymicrosin_{7-26}$ (sub-MIC to 2 × MIC) or polymyxin B (0.78 or 3.125 μg/mL). The fluorescence intensities, with excitation at 485 nm and emission at 525 nm, were continuously measured using a multimode microplate reader from Tecan, Switzerland. Each experiment was conducted independently three times.

Evaluation of the Permeability of MRSA Inner Membranes in the Presence of $Scymicrosin_{7-26}$. The effect of $Scymicrosin_{7-26}$ on the permeability of the bacterial inner membrane was assessed according to a previously reported method.[55] Briefly, logarithmically grown MRSA QZ19131 cultures were collected, washed three times in sodium phosphate buffer (pH 7.4) and then adjusted to 1 × 10^7 CFU/mL. Bacterial cultures were exposed to $Scymicrosin_{7-26}$ (2 × MIC or 4 × MIC) and incubated at 37 °C for 30 min. In parallel, a control bacterial suspension was prepared by mixing with Milli-Q water to serve as a negative control, while another was prepared with 2 μg/mL polymyxin B (PMB) to serve as a positive control. After three washes, the samples underwent staining with 2‰ SYTO 9 and propidium iodide (PI). The stained samples were then incubated at room temperature for 15 min in darkness to allow for staining to occur. Finally, the samples were analyzed using confocal laser scanning microscopy (CLSM, ZEISS LSM780, Germany). This experimental procedure was repeated three times to ensure reproducibility.

Scanning Electron Microscopy Observation. Sample preparation and processing were performed as previously reported with some modifications.[56] Briefly, 10^8 CFU/mL MRSA QZ19131 were suspended in MH broth and incubated with an equal volume of sterile water (control) or $Scymicrosin_{7-26}$ (2 × MIC or 4 × MIC) for 30 min. After incubation, the cell samples were rinsed three times with phosphate buffered saline (PBS) and then fixed for a long time in a 2.5% glutaraldehyde solution at 4 °C. Subsequently, the samples were washed again and mounted onto poly-L-lysine-coated glass slides to facilitate adherence. Dehydration of the samples was achieved through a series of graded ethanol treatments, after which they were dried and sputter-coated with gold particles. The samples were then visualized using a field emission scanning electron microscope (FEI Quanta 650 FEG, United States).[53] To ensure the reliability of the findings, the experiment was conducted independently on two separate occasions.

Transmission Electron Microscopy Observation. TEM samples were prepared as in the SEM procedure except that the bacterial concentration was 10-fold higher than that of the SEM sample.[56] Similarly, the cells were fixed using a 2.5% glutaraldehyde solution at 4 °C overnight. Following fixation, the cells were rinsed three times with PBS and then pre-embedded in a 2% agar solution. Subsequently, the samples underwent postfixation with 1% osmium tetroxide at 4 °C overnight. All samples were successively subjected to gradient ethanol dehydration, uranyl acetate staining, acetone rinsing and epoxy resin embedding procedures. Finally, ultrathin sections were made, subsequently stained, and subsequently observed under a transmission electron microscope (Hitachi HT-7800, Japan).

https://doi.org/10.1021/acsinfecdis.5c00034
ACS Infect. Dis. 2025, 11, 1216−1232

FITC-Scymicrosin$_{7-26}$ Targets MRSA. Binding properties of Scymicrosin$_{7-26}$ to MRSA was performed as previously described, with minor modifications.[17] Briefly, MRSA QZ19131 in the exponential growth phase was harvested and diluted to a final concentration of 10^9 CFU/mL, then incubated with an equal volume of FITC-Scymicrosin$_{7-26}$ (1 × MIC or 2 × MIC) for 30 min. The samples were rinsed and stained with DAPI for 15 min, followed by imaging using a laser confocal microscope (ZEISS, Germany).

Ion Tolerance, Thermal and Serum Stability of Scymicrosin$_{7-26}$. Peptide stability was assessed as described previously.[30,36,57] Briefly, MRSA QZ19131 in the exponential growth phase was harvested and diluted to a final concentration of 10^7 CFU/mL. To assess sodium ion and potassium ion tolerance, MRSA QZ19131 was cultivated in conjunction with Scymicrosin$_{7-26}$ in with varying NaCl (ranging from 0 to 300 mM) and KCl (ranging from 0 to 20 mM) concentrations. Optical density (OD) measurements at 595 nm were taken at intervals of 12 h at a temperature of 37 °C in a multimode microplate reader (Tecan, Switzerland).

Similarly, Scymicrosin$_{7-26}$ underwent heat treatment in a controlled water bath at 100 °C for various durations: 0, 10, 20, 30, 40, 50, 60, and 120 min. Following cooling, the treated Scymicrosin$_{7-26}$ was combined with a diluted bacterial suspension in microtiter plate wells and incubated at 37 °C. Absorbance measurements at 595 nm were taken at 12 h intervals using a multimode microplate reader.

To evaluate the serum stability of Scymicrosin$_{7-26}$, we measuered its antimicrobial activity under different serum conditions. Peptide solutions (0−48 μM) were preincubated with serially diluted serum (0, 1, 2.5, 5, 10, and 20% v/v) at 37 °C for 1 h to simulate physiological protease exposure. The antimicrobial efficacy was subsequently determined through MIC assays against MRSA using the broth microdilution. Experimental validation included three technical replicates for each condition and three independent replicates of the entire series to ensure statistical robustness.

Cytotoxicity Assay and Hemolytic Activity Assay. Human immortalized keratinocytes HaCaT was propagated in Dulbecco's modified Eagle medium (DMEM) supplemented with 10% fetal bovine serum (FBS). These cells were cultivated in a humidified incubator at 37 °C with an atmosphere of 5% CO_2. CellTiter 96 AQ_{ueous} assay (Promega, United States) was performed to determine cell viability.[16] The cells (1×10^4) were seeded into 96-well plates for 18−24 h, followed by the addition of fresh medium with or without Scymicrosin$_{7-26}$. After 24 h of incubation, the MTS-PMS reagent was added and incubated for an additional 1−4 h. Absorbance measurements were then taken at 492 nm using a multimode microplate reader.

The hemolytic activity was detected as previously reported.[56] After washing with 0.85% NaCl, 4% erythrocytes were incubated with Scymicrosin$_{7-26}$, 0.85% NaCl (negative control) or 1% TritonX-100 (positive control) at 37 °C for 1 h. The absorbance of the supernatants at 540 nm was determined using a multimode microplate reader (Tecan, Switzerland), and the hemolysis ratio was calculated as previously reported.[56] Each experiment was conducted independently three times.

Cell Membrane Penetration Activity of Scymicrosin$_{7-26}$. HaCaT cells were activated and passaged 2−3 times to achieve optimal cell condition. Cells were harvested, counted using a hemocytometer, and then seeded into a 96-well glass-bottom cell culture plate at a density of 3.0×10^4 cells per well for overnight incubation. FITC-labeled Scymicrosin$_{7-26}$ was diluted with serum-free DMEM to final concentrations of 1.5, 3, 6, 12, and 24 μM and then added to each well. Following a 1 h incubation, the cells were rinsed three times with PBS to eliminate any unbound Scymicrosin$_{7-26}$. Subsequently, the cells were fixed using a 4% (w/v) paraformaldehyde solution in PBS for 20 min to maintain their morphological structure. After fixation, the cells underwent permeabilization with a 0.1% (v/v) Triton X-100 solution in PBS for a duration of 10 min to facilitate the penetration of staining agents. After permeabilization, the cells were extensively rinsed with PBS three times to eliminate any remaining Triton X-100. The nuclei were stained with Hoechst 33,342 (excitation/emission maxima: 460/490 nm), and the cytoskeleton was labeled with rhodamine phalloidin (excitation/emission maxima: 540/565 nm). The stained cells were then observed under a confocal microscope to assess the internalization of Scymicrosin$_{7-26}$.

Evaluation of the Inhibitory Effect of Scymicrosin$_{7-26}$ Against MRSA Extracellular and Intracellular Infections. The antimicrobial efficacy of Scymicrosin$_{7-26}$ against MRSA in HaCaT cells was assessed using two different experimental designs to evaluate both the extracellular and intracellular bacterial loads.

Pretreatment with MRSA. HaCaT cells were first infected with MRSA QZ19131 at a concentration of 10^6 CFU/mL for 1 h and then the cells were exposed to Scymicrosin$_{7-26}$ at concentrations of 3, 6, 12, and 24 μM. After 12 h of incubation, the extracellular and intracellular bacterial loads were determined using a colony-forming unit (CFU) assay. The extracellular bacterial load was quantified by diluting the supernatant from each well and plating it on nutrient broth (NB) agar plates for colony counting.

The intracellular bacterial load was assessed with a modified protocol as previously described.[23] HaCaT cells were cultured in DMEM supplemented with 2% FBS, and approximately 40,000 cells were plated in 96-well plates and incubated overnight. MRSA QZ19131 in exponential growth phase were harvested, washed, and resuspended in serum-free DMEM. A 100 μL portion of this bacterial suspension, with a concentration of 10^6 CFU/mL, was dispensed into each well of the plate. Following a 1 h incubation at 37 °C within an atmosphere containing 5% CO_2, the cells were rinsed three times with PBS and exposed to 100 μg/mL gentamicin for 30 min to eliminate extracellular bacteria. After repeating the washing steps, 100 μL of serum-free DMEM with varying concentrations of Scymicrosin$_{7-26}$ was added to the wells. The cells were then further incubated for 12 h at 37 °C in a 5% CO_2 environment. Subsequent to this, the cells underwent three PBS rinses and were lysed using 0.1% Triton X-100 in PBS for a duration of 5 min. The resulting lysate was serially diluted and spread onto nutrient broth (NB) agar plates for colony enumeration. Each experimental step was performed in triplicate to ascertain the statistical validity of the results.

Pretreatment with Scymicrosin$_{7-26}$. HaCaT cells were pretreated with Scymicrosin$_{7-26}$ at concentrations of 3, 6, 12, and 24 μM for 1 h. After pretreatment, the cells were infected with MRSA QZ19131, and then the bacterial load was assessed using both extracellular and intracellular CFU assays after 12 h of incubation. The evaluation procedure was similar to the treatment described above, except that MRSA QZ19131 and Scymicrosin$_{7-26}$ were processed in reverse order.

https://doi.org/10.1021/acsinfecdis.5c00034
ACS Infect. Dis. 2025, 11, 1216−1232

***In Vivo* Toxicity of Scymicrosin$_{7-26}$.** Scymicrosin$_{7-26}$ is a peptide derived from *S. paramamosain*. Prior to conducting experiments in murine models, we performed comprehensive *in vivo* toxicity assessments using the marine medaka (*O. melastigma*) as a model organism. This species has been well-established as a reliable model for marine compound toxicity evaluation.[24] To evaluate the *in vivo* toxicity of Scymicrosin$_{7-26}$, healthy 3 month-old medaka with robust physique and uniform body size were selected for the experiment. The experimental design included a control group and Scymicrosin$_{7-26}$-treated group (1 and 2 mg/mL), with three replicates per group and 20 medaka in each group. The control group and the Scymicrosin$_{7-26}$-treated group were intraperitoneally injected with 8.8 μL of sterile water and the corresponding concentrations of Scymicrosin$_{7-26}$, respectively. During the experimental period, the fish were not fed. The vitality and mortality of the fish in the experimental and control groups were observed continuously, and the liver and intestinal tissues of the medaka were sampled at 48 and 96 h for histopathological examinations.

Establishment of a Mouse Model of MRSA Skin Wound Infection and Evaluation of the Therapeutic Efficacy of Scymicrosin$_{7-26}$. The establishment of a skin wound infection model in mice was conducted with a modification of the reported protocols.[58,59] Mice were rendered unconscious by intraperitoneal administration of avertin, procured from Sigma-Aldrich in the United States. The dorsal area of each mouse was shaved and two full-thickness excision wounds of 5 mm diameter each, were created using a biopsy punch. MRSA QZ19131, cultured to the mid logarithmic phase, was collected, rinsed, and then reconstituted in a 0.85% NaCl solution to achieve a concentration of 10^9 CFU/mL. A 25 μL aliquot of the bacterial suspension was applied to each wound, and the mice were allowed to be infected for 30 min before the initiation of treatment.

Mice were randomly allocated to one of three treatment groups. Hypromellose ointment was prepared following a previously described method.[45] Given that vancomycin is an FDA-approved antibiotic for the treatment of MRSA infections in traumatic wounds,[7] it was used as a positive control in this study. Wound infections were treated topically with either 2% hypromellose ointment containing sterile water (control group), 0.2% (w/w) Scymicrosin$_{7-26}$, or 0.1% (w/w) vancomycin. Additional treatments were administered at 12 h intervals on days 2 to 4. Photo documentation of the wound areas was conducted on days 1, 5, and 9 post-treatments. Subsequently, the digital images were processed with ImageJ software (National Institutes of Health, USA), to determine the wound area measurements. Finally, the wound shrinkage rate (WCR) is calculated according to the method described previously.[51]

For the bacterial load assessment, skin tissues were homogenized using an electric tissue homogenizer, and then the homogenate was serially diluted and spread onto nutrient broth (NB) agar plates for colony counting. This experiment was conducted in two independent trials to ensure reproducibility.

For histological examination, skin tissues were immersed in 4% formaldehyde solution for fixation, followed by embedding in paraffin, then sectionalized and stained with hematoxylin and eosin (H&E).

Statistical Analysis. All data were represented as mean ± standard error (SE). Two-way ANOVA or One-way ANOVA with Dunnett's posttest was used to analyze the significance of differences. p values < 0.05 were considered as statistically significant ($^*p < 0.05$, $^{**}p < 0.01$, $^{***}p < 0.001$).

■ ASSOCIATED CONTENT

Data Availability Statement

All pertinent data are included in the manuscript and the associated Supporting Information files. The full-length cDNA sequence of Scymicrosin can be accessed in the NCBI database under the GenBank Accession Number OP382459.

■ AUTHOR INFORMATION

Corresponding Authors

Fangyi Chen − *State Key Laboratory of Marine Environmental Science, College of Ocean and Earth Sciences, Xiamen University, Xiamen 361005, China; State-Province Joint Engineering Laboratory of Marine Bioproducts and Technology, College of Ocean and Earth Sciences and Fujian Innovation Research Institute for Marine Biological Antimicrobial Peptide Industrial Technology, College of Ocean & Earth Sciences, Xiamen University, Xiamen 361005, China*; Email: chenfangyi@xmu.edu.cn

Ke-Jian Wang − *State Key Laboratory of Marine Environmental Science, College of Ocean and Earth Sciences, Xiamen University, Xiamen 361005, China; State-Province Joint Engineering Laboratory of Marine Bioproducts and Technology, College of Ocean and Earth Sciences and Fujian Innovation Research Institute for Marine Biological Antimicrobial Peptide Industrial Technology, College of Ocean & Earth Sciences, Xiamen University, Xiamen 361005, China*; Email: wkjian@xmu.edu.cn

Authors

Ying Zhou − *State Key Laboratory of Marine Environmental Science, College of Ocean and Earth Sciences, Xiamen University, Xiamen 361005, China; State-Province Joint Engineering Laboratory of Marine Bioproducts and Technology, College of Ocean and Earth Sciences, Xiamen University, Xiamen 361005, China*

Ying Wang − *State Key Laboratory of Marine Environmental Science, College of Ocean and Earth Sciences, Xiamen University, Xiamen 361005, China; State-Province Joint Engineering Laboratory of Marine Bioproducts and Technology, College of Ocean and Earth Sciences, Xiamen University, Xiamen 361005, China;* orcid.org/0000-0002-0431-7289

Xiangyu Meng − *State Key Laboratory of Marine Environmental Science, College of Ocean and Earth Sciences, Xiamen University, Xiamen 361005, China; State-Province Joint Engineering Laboratory of Marine Bioproducts and Technology, College of Ocean and Earth Sciences, Xiamen University, Xiamen 361005, China*

Ming Xiong − *State Key Laboratory of Marine Environmental Science, College of Ocean and Earth Sciences, Xiamen University, Xiamen 361005, China; State-Province Joint Engineering Laboratory of Marine Bioproducts and Technology, College of Ocean and Earth Sciences and Fujian Innovation Research Institute for Marine Biological Antimicrobial Peptide Industrial Technology, College of Ocean & Earth Sciences, Xiamen University, Xiamen 361005, China*

Xianxian Dong − *State Key Laboratory of Marine Environmental Science, College of Ocean and Earth Sciences,*

https://doi.org/10.1021/acsinfecdis.5c00034
ACS Infect. Dis. 2025, 11, 1216−1232

Xiamen University, Xiamen 361005, China; State-Province Joint Engineering Laboratory of Marine Bioproducts and Technology, College of Ocean and Earth Sciences, Xiamen University, Xiamen 361005, China

Hui Peng − *State Key Laboratory of Marine Environmental Science, College of Ocean and Earth Sciences, Xiamen University, Xiamen 361005, China; State-Province Joint Engineering Laboratory of Marine Bioproducts and Technology, College of Ocean and Earth Sciences and Fujian Innovation Research Institute for Marine Biological Antimicrobial Peptide Industrial Technology, College of Ocean & Earth Sciences, Xiamen University, Xiamen 361005, China*

Complete contact information is available at: https://pubs.acs.org/10.1021/acsinfecdis.5c00034

Author Contributions

‖Y.Z. and Y.W. authors contributed equally to this work. **Ying Zhou:** data curation, investigation, methodology, software, validation, visualization, writing—original draft. **Ying Wang:** data curation, formal analysis, methodology, validation, visualization, writing—original draft, writing—review and editing. **Xiangyu Meng:** investigation, methodology. **Ming Xiong:** investigation, methodology. **Xianxian Dong:** investigation, methodology. **Hui Peng:** investigation, methodology. **Fangyi Chen:** conceptualization, funding acquisition, project administration, resources, supervision, writing—review and editing. **Ke-Jian Wang:** conceptualization, funding acquisition, project administration, resources, supervision, writing—review and editing.

Funding

This study was supported by grant 42376089/U1805233/41806162 from the National Natural Science Foundation of China; grant FJHY-YYKJ-2022-1-14 from Fujian Ocean and Fisheries Bureau; grant FOCAL2023-0207 from Fujian Ocean Synergy Alliance (FOCAL) and grant 22CZP002HJ08 from Xiamen Ocean Development Bureau.

Notes

The authors declare no competing financial interest.

■ ACKNOWLEDGMENTS

We express our gratitude to the Second Affiliated Hospital of Fujian Medical University (Quanzhou, Fujian, China) for supplying the clinical isolates. We also extend our thanks to laboratory engineers Huiyun Chen and Zhiyong Lin for their valuable technical support.

■ REFERENCES

(1) Mwangi, J.; Hao, X.; Lai, R.; Zhang, Z. Y. Antimicrobial peptides: new hope in the war against multidrug resistance. *Zool. Res.* **2019**, *40* (6), 488−505.

(2) Hutchings, M. I.; Truman, A. W.; Wilkinson, B. Antibiotics: past, present and future. *Curr. Opin. Microbiol.* **2019**, *51*, 72−80.

(3) Aslam, B.; Wang, W.; Arshad, M. I.; Khurshid, M.; Muzammil, S.; Rasool, M. H.; Nisar, M. A.; Alvi, R. F.; Aslam, M. A.; Qamar, M. U.; Salamat, M. K. F.; Baloch, Z. Antibiotic resistance: a rundown of a global crisis. *Infect. Drug Resist.* **2018**, *11*, 1645−1658.

(4) O'Neill, J. *Antimicrobial resistance: tackling a crisis for the health and wealth of nations*, 2014.

(5) Santajit, S.; Indrawattana, N. Mechanisms of antimicrobial resistance in ESKAPE pathogens. *Biomed Res. Int.* **2016**, *2016*, 1−8.

(6) Simonetti, O.; Lucarini, G.; Morroni, G.; Orlando, F.; Lazzarini, R.; Zizzi, A.; Brescini, L.; Provinciali, M.; Giacometti, A.; Offidani, A.; Cirioni, O. New evidence and insights on dalbavancin and wound healing in a mouse model of skin infection. *Antimicrob. Agents Chemother.* **2020**, *64* (4), 020622-19.

(7) Liu, C.; Bayer, A.; Cosgrove, S. E.; Daum, R. S.; Fridkin, S. K.; Gorwitz, R. J.; Kaplan, S. L.; Karchmer, A. W.; Levine, D. P.; Murray, B. E.; Rybak, M. J.; Talan, D. A.; Chambers, H. F. Clinical practice guidelines by the infectious diseases society of America for the treatment of methicillin-resistant *Staphylococcus aureus* infections in adults and children. *Clin. Infect. Dis.* **2011**, *52* (3), e18−e55.

(8) Tacconelli, E.; Carrara, E.; Savoldi, A.; Harbarth, S.; Mendelson, M.; Monnet, D. L.; Pulcini, C.; Kahlmeter, G.; Kluytmans, J.; Carmeli, Y.; Ouellette, M.; Outterson, K.; Patel, J.; Cavaleri, M.; Cox, E. M.; Houchens, C. R.; Grayson, M. L.; Hansen, P.; Singh, N.; Theuretzbacher, U.; Magrini, N.; Aboderin, A. O.; et al. Discovery, research, and development of new antibiotics: the WHO priority list of antibiotic-resistant bacteria and tuberculosis. *Lancet Infect. Dis.* **2018**, *18* (3), 318−327.

(9) Desbois, A. P.; Gemmell, C. G.; Coote, P. J. *In vivo* efficacy of the antimicrobial peptide ranalexin in combination with the endopeptidase lysostaphin against wound and systemic meticillin-resistant *Staphylococcus aureus* (MRSA) infections. *Int. J. Antimicrob. Agents* **2010**, *35* (6), 559−565.

(10) Ma, Z.; Han, J. Z.; Chang, B. X.; Gao, L.; Lu, Z. X.; Lu, F. X.; Zhao, H. Z.; Zhang, C.; Bie, X. M. Membrane-active amphipathic peptide WRL3 with *in vitro* antibiofilm capability and *in vivo* efficacy in treating methicillin-resistant *Staphylococcus aureus* burn wound infections. *ACS Infect. Dis.* **2017**, *3* (11), 820−832.

(11) Starr, C. G.; Ghimire, J.; Guha, S.; Hoffmann, J. P.; Wang, Y. H.; Sun, L. S.; Landreneau, B. N.; Kolansky, Z. D.; Kilanowski-Doroh, I. M.; Sammarco, M. C.; Morici, L. A.; Wimley, W. C. Synthetic molecular evolution of host cell-compatible, antimicrobial peptides effective against drug-resistant, biofilm-forming bacteria. *Proc. Natl. Acad. Sci. U.S.A.* **2020**, *117* (15), 8437−8448.

(12) Pfalzgraff, A.; Brandenburg, K.; Weindl, G. Antimicrobial peptides and their therapeutic potential for bacterial skin infections and wounds. *Front. Pharmacol* **2018**, *9*, 281.

(13) Brogden, K. A. Antimicrobial peptides: pore formers or metabolic inhibitors in bacteria? *Nat. Rev. Microbiol.* **2005**, *3* (3), 238−250.

(14) Struyfs, C.; Cammue, B. P. A.; Thevissen, K. Membrane-interacting antifungal peptides. *Front. Cell Dev. Biol.* **2021**, *9*, 649875.

(15) Zanjani, N. T.; Miranda-Saksena, M.; Cunningham, A. L.; Dehghani, F. Antimicrobial peptides of Marine crustaceans: the potential and challenges of developing therapeutic agents. *Curr. Med. Chem.* **2018**, *25* (19), 2245−2259.

(16) Yang, Y.; Chen, F.; Chen, H.-Y.; Peng, H.; Hao, H.; Wang, K.-J. A novel antimicrobial peptide Scyreprocin from mud crab *Scylla paramamosain* showing potent antifungal and anti-biofilm activity. *Front. Microbiol.* **2020**, *11*, 1589.

(17) Chen, Y. C.; Yang, Y.; Zhang, C.; Chen, H. Y.; Chen, F. Y.; Wang, K. J. A novel antimicrobial peptide Sparamosin$_{26-54}$ from the mud crab *Scylla paramamosain* showing potent antifungal activity against *Cryptococcus neoformans*. *Front. Microbiol.* **2021**, *12*, 746006.

(18) Jiang, M. Y.; Chen, R. S.; Zhang, J. R.; Chen, F. Y.; Wang, K. J. A novel antimicrobial peptide Spampcin$_{56-86}$ from exerting rapid bactericidal and anti-biofilm activity *in vitro* and anti-infection *in vivo*. *Int. J. Mol. Sci.* **2022**, *23* (21), 13316.

(19) Koo, H. B.; Seo, J. Antimicrobial peptides under clinical investigation. *Pept. Sci.* **2019**, *111* (5), No. e24122.

(20) Mookherjee, N.; Anderson, M. A.; Haagsman, H. P.; Davidson, D. J. Antimicrobial host defence peptides: functions and clinical potential. *Nat. Rev. Drug Discovery* **2020**, *19* (5), 311−332.

(21) Mahlapuu, M.; Björn, C.; Ekblom, J. Antimicrobial peptides as therapeutic agents: opportunities and challenges. *Crit. Rev. Biotechnol.* **2020**, *40* (7), 978−992.

(22) Håkansson, J.; Ringstad, L.; Umerska, A.; Johansson, J.; Andersson, T.; Boge, L.; Rozenbaum, R. T.; Sharma, P. K.; Tollbäck, P.; Björn, C.; Saulnier, P.; Mahlapuu, M. Characterization of the *in vitro, ex vivo*, and *in vivo* efficacy of the antimicrobial peptide DPK-

060 used for topical treatment. *Front. Cell. Infect. Microbiol.* **2019**, *9*, 174.
(23) Di Grazia, A.; Luca, V.; Segev-Zarko, L.-a. T.; Shai, Y.; Mangoni, M. L. Temporins A and B stimulate migration of HaCaT keratinocytes and kill intracellular *Staphylococcus aureus*. *Antimicrob. Agents Chemother.* **2014**, *58* (5), 2520−2527.
(24) Xinlong, W.; Qiansheng, H.; Chao, F.; Sijun, D. Oryzias melastigma: A New Promising Model Organism for Marine Ecotoxicology. *Asian J. Ecotoxicol.* **2012**, *07* (4), 345−353.
(25) Allen, H. K.; Trachsel, J.; Looft, T.; Casey, T. A. Finding alternatives to antibiotics. *Antimicrobial Ther. Rev.* **2014**, *1323*, 91−100.
(26) Rima, M.; Rima, M.; Fajloun, Z.; Sabatier, J. M.; Bechinger, B.; Naas, T. Antimicrobial peptides: a potent alternative to antibiotics. *Antibiotics-Basel* **2021**, *10* (9), 1095.
(27) Kumar, P.; Kizhakkedathu, J. N.; Straus, S. K. Antimicrobial peptides: diversity, mechanism of action and strategies to improve the activity and biocompatibility *in vivo*. *Biomolecules* **2018**, *8* (1), 4.
(28) Ciumac, D.; Gong, H. N.; Hu, X. Z.; Lu, J. R. Membrane targeting cationic antimicrobial peptides. *J. Colloid Interface Sci.* **2019**, *537*, 163−185.
(29) Stone, T. A.; Cole, G. B.; Ravamehr-Lake, D.; Nguyen, H. Q.; Khan, F.; Sharpe, S.; Deber, C. M. Positive charge patterning and hydrophobicity of membrane-active antimicrobial Peptides as determinants of activity, toxicity, and pharmacokinetic stability. *J. Med. Chem.* **2019**, *62* (13), 6276−6286.
(30) Bai, Y. Q.; Zhang, W. B.; Zheng, W. B.; Meng, X. Z.; Duan, Y. Y.; Zhang, C.; Chen, F. Y.; Wang, K. J. A 14-amino acid cationic peptide Bolespleenin$_{334-347}$ from the marine fish *mudskipper Boleophthalmus pectinirostris* exhibiting potent antimicrobial activity and therapeutic potential. *Biochem. Pharmacol.* **2024**, *226*, 116344.
(31) Wang, X.; Hong, X.; Chen, F.; Wang, K. A truncated peptide Spgillcin$_{177-189}$ derived from mud crab *Scylla paramamosain* exerting multiple antibacterial activities. *Front. Cell. Infect. Microbiol.* **2022**, *12*, 928220.
(32) Chen, P.; Ye, T.; Li, C.; Praveen, P.; Hu, Z.; Li, W.; Shang, C. Embracing the era of antimicrobial peptides with marine organisms. *Nat. Prod. Rep.* **2024**, *41* (3), 331−346.
(33) Fjell, C. D.; Hiss, J. A.; Hancock, R. E. W.; Schneider, G. Designing antimicrobial peptides: form follows function. *Nat. Rev. Drug Discovery* **2012**, *11* (1), 37−51.
(34) Han, Y. J.; Zhang, M. L.; Lai, R.; Zhang, Z. Y. Chemical modifications to increase the therapeutic potential of antimicrobial peptides. *Peptides* **2021**, *146*, 170666.
(35) Lima, A. M.; Azevedo, M. I. G.; Sousa, L. M.; Oliveira, N. S.; Andrade, C. R.; Freitas, C. D. T.; Souza, P. F. N. Plant antimicrobial peptides: An overview about classification, toxicity and clinical applications. *Int. J. Biol. Macromol.* **2022**, *214*, 10−21.
(36) Shang, L.; Wu, Y.; Wei, N.; Yang, F.; Wang, M.; Zhang, L.; Fei, C.; Liu, Y.; Xue, F.; Gu, F. Novel Arginine End-Tagging Antimicrobial Peptides to Combat Multidrug-Resistant Bacteria. *ACS Appl. Mater. Interfaces* **2021**, *14* (1), 245−258.
(37) Cutrona, K. J.; Kaufman, B. A.; Figueroa, D. M.; Elmore, D. E. Role of arginine and lysine in the antimicrobial mechanism of histone-derived antimicrobial peptides. *FEBS Lett.* **2015**, *589* (24), 3915−3920.
(38) Tang, W.-H.; Wang, C.-F.; Liao, Y.-D. Fetal bovine serum albumin inhibits antimicrobial peptide activity and binds drug only in complex with α1-antitrypsin. *Sci. Rep.* **2021**, *11* (1), 1267.
(39) Arnab, M. K. H.; Hasan, M.; Islam, M. M. An Insight into the Structure-Activity Relationship of Antimicrobial Peptide Brevinin. *J. Pharm. Sci.* **2023**, *16* (4), 815−829.
(40) Bird, G. H.; Madani, N.; Perry, A. F.; Princiotto, A. M.; Supko, J. G.; He, X. Y.; Gavathiotis, E.; Sodroski, J. G.; Walensky, L. D. Hydrocarbon double-stapling remedies the proteolytic instability of a lengthy peptide therapeutic. *Proc. Natl. Acad. Sci. U.S.A.* **2010**, *107* (32), 14093−14098.
(41) Buccini, D. F.; Cardoso, M. H.; Franco, O. L. Antimicrobial peptides and cell-penetrating peptides for treating intracellular bacterial infections. *Front. Cell. Infect. Microbiol.* **2021**, *10*, 612931.
(42) Chung, E. M. C.; Dean, S. N.; Propst, C. N.; Bishop, B. M.; van Hoek, M. L. Komodo dragon-inspired synthetic peptide DRGN-1 promotes wound-healing of a mixed-biofilm infected wound. *npj Biofilms Microbiomes* **2017**, *3*, 9.
(43) Jung Kim, D.; Lee, Y. W.; Park, M. K.; Shin, J. R.; Lim, K. J.; Cho, J. H.; Kim, S. C. Efficacy of the designer antimicrobial peptide SHAP1 in wound healing and wound infection. *Amino Acids* **2014**, *46* (10), 2333−2343.
(44) Simoes, D.; Miguel, S. P.; Ribeiro, M. P.; Coutinho, P.; Mendonça, A. G.; Correia, I. J. Recent advances on antimicrobial wound dressing: A review. *Eur. J. Pharm. Biopharm.* **2018**, *127*, 130−141.
(45) Haisma, E. M.; Göblyös, A.; Ravensbergen, B.; Adriaans, A. E.; Cordfunke, R. A.; Schrumpf, J.; Limpens, R. W. A. L.; Schimmel, K. J. M.; den Hartigh, J.; Hiemstra, P. S.; Drijfhout, J. W.; El Ghalbzouri, A.; Nibbering, P. H. Antimicrobial peptide P60.4Ac-containing creams and gel for eradication of methicillin-resistant from cultured skin and airway epithelial surfaces. *Antimicrob. Agents Chemother.* **2016**, *60* (7), 4063−4072.
(46) de Breij, A.; Riool, M.; Cordfunke, R. A.; Malanovic, N.; de Boer, L.; Koning, R. I.; Ravensbergen, E.; Franken, M.; van der Heijde, T.; Boekema, B. K.; Kwakman, P. H. S.; Kamp, N.; El Ghalbzouri, A.; Lohner, K.; Zaat, S. A. J.; Drijfhout, J. W.; Nibbering, P. H. The antimicrobial peptide SAAP-148 combats drug-resistant bacteria and biofilms. *Sci. Transl. Med.* **2018**, *10* (423), No. eaan4044.
(47) Perez-Robles, S.; Carotenuto, C.; Minale, M. HPMC Hydrogel Formation Mechanisms Unveiled by the Evaluation of the Activation Energy. *Polymers* **2022**, *14* (3), 635.
(48) Piotrowska, U.; Sobczak, M.; Oledzka, E. Current state of a dual behaviour of antimicrobial peptides—Therapeutic agents and promising delivery vectors. *Chem. Biol. Drug Des.* **2017**, *90* (6), 1079−1093.
(49) Ron-Doitch, S.; Sawodny, B.; Kühbacher, A.; David, M. M. N.; Samanta, A.; Phopase, J.; Burger-Kentischer, A.; Griffith, M.; Golomb, G.; Rupp, S. Reduced cytotoxicity and enhanced bioactivity of cationic antimicrobial peptides liposomes in cell cultures and 3D epidermis model against HSV. *J. Controlled Release* **2016**, *229*, 163−171.
(50) Kumar, P.; Pletzer, D.; Haney, E. F.; Rahanjam, N.; Cheng, J. T. J.; Yue, M.; Aljehani, W.; Hancock, R. E. W.; Kizhakkedathu, J. N.; Straus, S. K. Aurein-derived antimicrobial peptides formulated with pegylated phospholipid micelles to target methicillin-resistant skin infections. *ACS Infect. Dis.* **2019**, *5* (3), 443−453.
(51) Bahreini, M.; Moghaddam, M. M.; Ghorbani, M.; Nourani, M. R.; Mirnejad, R. Antimicrobial peptide-fibrin glue mixture for treatment of methicillin-resistant *Staphylococcus aureus*-infected wounds. *Ther. Delivery* **2024**, *15* (8), 577−591.
(52) Zhu, Y. Y.; Hao, W. J.; Wang, X.; Ouyang, J. H.; Deng, X. Y.; Yu, H. N.; Wang, Y. P. Antimicrobial peptides, conventional antibiotics, and their synergistic utility for the treatment of drug-resistant infections. *Med. Res. Rev.* **2022**, *42* (4), 1377−1422.
(53) Zhou, Y.; Meng, X. Y.; Chen, F. Y.; Xiong, M.; Zhang, W. B.; Wang, K. J. Newly discovered antimicrobial peptide Scyampcin$_{44-63}$ from *Scylla paramamosain* exhibits a multitargeted candidacidal mechanism *in vitro* and is effective in a murine model of vaginal candidiasis. *Antimicrob. Agents Chemother.* **2023**, *67* (6), No. e00022-00023.
(54) Zhang, W. B.; An, Z.; Bai, Y. Q.; Zhou, Y.; Chen, F. Y.; Wang, K. J. A novel antimicrobial peptide Scyreptin$_{1-30}$ from *Scylla paramamosain* exhibiting potential therapy of *Pseudomonas aeruginosa* early infection in a mouse burn wound model. *Biochem. Pharmacol.* **2023**, *218*, 115917.
(55) Zhang, W.; An, Z.; Bai, Y.; Zhou, Y.; Chen, F.; Wang, K.-J. A novel antimicrobial peptide Scyreptin$_{1-30}$ from *Scylla paramamosain* exhibiting potential therapy of *Pseudomonas aeruginosa* early infection

https://doi.org/10.1021/acsinfecdis.5c00034
ACS Infect. Dis. 2025, 11, 1216−1232

in a mouse burn wound model. *Biochem. Pharmacol.* **2023**, *218*, 115917.
(56) Zhu, D. P.; Chen, F. Y.; Chen, Y. C.; Peng, H.; Wang, K. J. The long-term effect of a nine amino-acid antimicrobial peptide AS-hepc3$_{(48-56)}$ against *Pseudomonas aeruginosa* With no detectable resistance. *Front. Cell. Infect. Microbiol.* **2021**, *11*, 752637.
(57) Zhang, C.; Chen, F. Y.; Bai, Y. Q.; Dong, X. X.; Meng, X. Z.; Wang, K. J. A novel antimicrobial peptide Spasin$_{141-165}$ identified from *Scylla paramamosain* exhibiting protection against *Aeromonas hydrophila* infection. *Aquaculture* **2024**, *591*, 741137.
(58) van Staden, A. D. P.; Heunis, T.; Smith, C.; Deane, S.; Dicks, L. M. T. Efficacy of lantibiotic treatment of *Staphylococcus aureus*-induced skin infections, monitored by *in vivo* bioluminescent imaging. *Antimicrob. Agents Chemother.* **2016**, *60* (7), 3948−3955.
(59) Huang, H. N.; Rajanbabu, V.; Pan, C. Y.; Chan, Y. L.; Wu, C. J.; Chen, J. Y. Use of the antimicrobial peptide Epinecidin-1 to protect against MRSA infection in mice with skin injuries. *Biomaterials* **2013**, *34* (38), 10319−10327.

https://doi.org/10.1021/acsinfecdis.5c00034
ACS Infect. Dis. 2025, 11, 1216−1232